



FACULTY OF SCIENCE AND TECHNOLOGY

MASTER'S THESIS

Study program/specialization:

Spring semester, 2021

MSc. Petroleum engineering/Natural Gas

Open access

Author: Elnur Gurzaliyev

Faculty supervisor: Prof. Steinar Evje

External supervisor: Research Prof. Ingebret Fjelde

Title of master's thesis:

Blocking of fracture by Laponite/HPAM gels: Experiments and simulations

Credits: 30 ECTS

Keywords:

Nanocomposite gels

Polymer

Laponite clay

IORCoresim

Number of pages:69

Stavanger, 14th June 2021

Acknowledgement

My deepest gratitude to my supervisor, Professor Ingebret Fjelde, for providing me with the opportunity to work on my thesis and for his advice during the process. I am grateful for the assistance and guidance provided by the outstanding people at NORCE, especially Dr Arouture Omekeh, for the simulation software.

I also appreciate my friends Joshgun Jafarguluzade and Gunel Ismayilova for their support.

Abstract

Water production is the primary obstacle for oil recovery with water injection from heterogeneous reservoirs with high-permeability streaks and fractures. The practical approach to solve the adverse effects of water flooding and better nanoparticle gel treatments intended for use as an ultimate objective of this research. Various concentrations of Laponite clay and HPAM interactions with different shut-in periods are simulated to examine the gel-forming.

Both laboratory experiments and simulations were carried out. First, three different gels were created by changing the concentration of gel components. Then, based on laboratory experiments and the literature, four different gel systems were acquired and used as the basis for the simulations.

The results showed that 2 % Laponite and 0.3 % HPAM interaction is a promising option for gel treatment. Gelation time was calculated for all cases, and it concluded that gelation time is high at low Laponite clay concentration. Gelation time should be less than the shut-in period; thus, gelation happens in the core plug. According to this research, gel treatment with a concentration of 2 % clay and 0.3 % polymer showed promise results of increasing oil recovery.

Laponite-HPAM interaction in fractured core plugs can be simulated using IORCoreSim. It concluded that the shut-in period should be more than gelation time to form a gel.

De-ionized water was used as the base for gel components in this thesis, and the further test could be carried out to see the effectiveness of seawater for gel-forming.

Contents

Acknowledgement	ii
Abstract	iii
List of figures.....	vii
List of tables	ix
Nomenclature.....	x
Chapter 1 Introduction	1
1.1 Statement and significance of the problem	1
1.2 Motivation and Objectives	2
1.3 Scope of work.....	3
Chapter 2 Literature review	4
2.1 Stages of oil production from a reservoir	4
2.1.1 Limitations of the secondary oil recovery.....	4
2.2 Enhanced Oil Recovery	5
2.2.1 Enhanced oil recovery methods.....	5
2.2.2 Chemical EOR.....	6
2.3 Polymer flooding and Rheology	7
2.4 Functions of nanomaterials in nano-flooding	10
2.4.1 Wettability alteration	10
2.4.2 Reduction of IFT	11
2.4.3 Controllable viscosity	12
2.4.4 Factors controlling the success of Nano flooding	12
2.5 Morphology of nanoparticle.....	12
2.6 Polymer gels.....	13
2.6.1 In-situ Gel (Traditional method)	14
2.6.2 Preformed gel systems	14

2.6.3 Bright water.....	15
2.6.4 Microgel.....	16
2.6.5 Preformed particle gel (PPG)	17
2.6.6 pH-sensitive polymer	18
2.7 Simulation of gelation and gel placement.....	19
2.8 Laponite clay.....	21
Chapter 3 Experimental and simulation methods	23
3.1 Chemicals.....	23
3.1.1 Polymer	23
3.1.2 Clay.....	23
3.2 Equipment/Materials	23
3.3 Characterisation of Laponite-HPAM interactions.....	24
3.4 Examination of Laponite-polymer gelation properties.....	24
3.5 Simulation Part.....	25
3.5.1 IORCORESIM: Mathematical Model	25
3.5.2 Simulation Input	26
3.5.3 Grid Description	26
3.5.4 Well Information	27
3.6 Gel time calculation.....	27
Chapter 4 Result and Discussion	29
4.1 Experiments	29
4.1.1 Characterisation of laponite gels in Deionized water	29
4.2 Gelation time	30
4.3 Simulations	31
4.3.1 Base case	32
4.3.2 Case: Without gel	37

4.3.3 Effect of concentration.....	40
4.3.3.1 Case 1 Laponite 1.5 % and HPAM 0.3%	40
4.3.3.2 Case 2 Laponite 1.0 % and HPAM 0.3%	41
4.3.3.3 Case 3 Laponite 1.0 % and HPAM 0.03%	43
4.3.4 Effect of shut-in period	44
4.3.4.1 Case 4 Shut-in 5 hours	44
4.3.4.2 Case 5 Shut-in 36 hours	46
4.3.5 Recovery factor affected by gel treatment for each case	47
4.4 Gel in the core	49
4.5 Discussion	50
4.6 Further work.....	51
Chapter 5 Conclusions	52
References	53

List of figures

Figure 2.1 Enhanced oil recovery methods(Vishnyakov et al., 2019).....	6
Figure 2.2 Left, using of inappropriate polymer creates fingering effect. Right, using appropriate polymer pushes all the petroleum towards the production well (Zerkhalov, 2015).	8
Figure 2.3 Viscosity model of a nonnewtonian fluid (Zerkhalov, 2015).....	8
Figure 2.4 Showing oil wettability of the reservoir (left). Increase in water wettability after injection of EOR fluids(Maghzi et al., 2011).	11
Figure 2.5 Mechanism of Aggregation in nanoparticles (Al-Hajri et al., 2018)	13
Figure 2.6 Gel composition (Imqam, 2015)	14
Figure 2.7 A summary of preformed gel systems (Imqam, 2015).....	15
Figure 2.8 Mode of activation of the particulate reagent (Imqam, 2015)	16
Figure 2.9 Microgel particles (van der Schaaf et al., 2016)	17
Figure 2.10 PPG particle before and after swell (Imqam et al., 2017)	18
Figure 2.11 Swelling of Polyacrylic acid swelling within ionization (Al-Anazi and Sharma, 2002)	18
Figure 3.1 Core view from the top.....	26
Figure 3.2 View of wells from top.....	27
Figure 4.1. Characterisation of gel code (Skrettingland et al., 2014)	29
Figure 4.2 Production rates for base case.....	32
Figure 4.3 Gel components versus pore volume in production	33
Figure 4.4 Cross-section from top: Gel in the core in different type steps	34
Figure 4.5 Cross-section from top: Oil saturation for Base case	35
Figure 4.6 Cross-section from top: Water permeability reduction	36

Figure 4.7 Production rates for Case: without gel	37
Figure 4.8 Cross-section from top: Oil saturation for Case: without gel	38
Figure 4.9 Cross-section from top: Oil saturation: Left side is Base case; Right side is Case: without gel	39
Figure 4.10 Production rates for Case 1	40
Figure 4.11 Gel components versus pore volume in production	41
Figure 4.12 Production rate for Case 2	42
Figure 4.13 Gel components versus pore volume in production	42
Figure 4.14 Production rates for Case 3.....	43
Figure 4.15 Gel components versus pore volume in production	44
Figure 4.16 Production rates for Case 4.....	45
Figure 4.17 Gel components versus pore volume in production	45
Figure 4.18 Production rates for Case 5.....	46
Figure 4.19 Gel components versus pore volume in production	47
Figure 4.20 Recovery factors for all cases in different pore volume Base case (clay 2% and polymer 0.3%) Case 1 (clay 1.5% and polymer 0.3) Case 2 (clay 1% and polymer 0.3) Case 3 (clay 1% and polymer 0.03) Case 4 decreased shut in time to 5hours Case 5 increased shut in time to 36hours	48
Figure 4.21 Pressure drop for all cases Base case (clay 2% and polymer 0.3%) Case 1 (clay 1.5% and polymer 0.3) Case 2 (clay 1% and polymer 0.3) Case 3 (clay 1% and polymer 0.03) Case 4 decreased shut in time to 5hours Case 5 increased shut in time to 36hours	49
Figure 4.22 Cross-section from top: A- Base Case B- Case 1 C- Case: No gel D- Case 5 at the end of the production	50

List of tables

Table 4.1 Investigation of Laponite-HPAM interactions in deionized water, heated at 50°C.	30
Table 4.2 Gel Model	30
Table 4.3 Gel components	31
Table 4.4 Gelation time	31

Nomenclature

3D	3-Dimensional
A_g	Adsorbed gel
C_{gcr}	Critical gel concentration
C_L	Laponite concentration
COBR	Crude Oil Brine – Rock
C_s	Salt concentration
EOR	Enhanced oil recovery
HPAM	Hydrolysed polyacrylamide
IFT	Interfacial tension
k	Reaction rate
k_r	Relative permeability
LCFG	Low concentration flowing gel
NC	Nanocomposite gels
NCS	Norwegian Continental Shelf
NPD	Norwegian Petroleum Directorate
OOIP	Original oil in place
P_c	Capillary pressure
PPG	Preformed particle gel
PV	Pro-vesicular
R	Gas constant
r_g	Correlation coefficient
T	Temperature
WSO	Water shutoff
wt %	Percentage by Weight

Chapter 1 Introduction

1.1 Statement and significance of the problem

The distributions of porosity, permeability, deposition and natural fractures are geological complications in the oil reservoirs (Lee and Lee, 2013). Permeability is the essential element for reservoir engineering calculations among numerous heterogeneous petrophysical parameters. Compared to a homogeneous permeability system, a heterogeneous permeability system causes various flows in the reservoir (Ahmadi and Chen, 2019).

The flow mechanism becomes more complex as the variability of the permeability distribution increases (Zamani et al., 2015). Therefore, even though the reservoir's average permeability is the same, permeability distribution leads to drastically differing improved oil recovery performance. It infers that a large amount of recoverable oil is left inside the reservoir. Sometimes, recovery factors concerning primary and secondary recovery stages do not go beyond 10-40% of OOIP (Zamani et al., 2015).

Based on the several types of research carried out, polymer solution became known as a mature and successful EOR process (Delshad et al., 2008)

Nanocomposite gel reduces excessive water production by boosting volumetric sweep efficiency, mainly vertical sweep efficiency. Polymer and cross-linker are used in the gel treatment (Guo et al., 2017). Because of the strong gel created by the large volume of the polymer network, it is difficult to flow through tiny pores in the matrix. Therefore, the bulk gel is used to treat high-permeability zones around wellbores or reservoirs with fractures because of its slow flow capacity. In-situ microgels are made with a low concentration of polymer and cross-linker. Until its gelation mechanism is started, the microgel can penetrate deeper into a formation. As a result, it is suitable for reservoirs with deep high-permeability zones or those without fractures. The in-situ microgels are chosen because the randomly heterogeneous reservoirs studied in this work have varied high-permeability zones without fractures. (Chauveteau et al., 2003).

1.2 Motivation and Objectives

Nanofluid injections into oil reservoirs can produce more than 50% of in-place oil reserves (Vishnyakov et al., 2019). However, this is not achievable by conventional methods (primary and secondary) or even by polymers. Therefore, nanofluid flooding is a very crucial EOR method where nanomaterial or nanocomposite fluids are introduced into the oil reservoirs to have an impact on the oil displacement or ameliorate injection (Fletcher and Davis, 2010) (Kong and Ohadi, 2010) (El-Diasty and Aly, 2015). Conventional EOR methods consist of thermal, chemical, microbial, miscible, and immiscible gas techniques. However, according to the various surveys carried out, chemical EOR involving polymers, surfactants, or alkalis is also considered a favourable technique to enhance sweep efficiency and oil displacement (J.Sheng, 2013).

Nonetheless, chemical EOR techniques can recover approximately 50% (In the laboratory, up to 100% if residual oil saturation is reduced oil reserves (McElfresh et al., 2012). Thus, we deem a technical review on technology innovations such as nano flooding could avail both academia and upstream industry. In comparison to conventional chemical flooding, nano flooding has excellent advantages. Nanomaterials can trigger additional functions by modifying material surface or switching template materials, such as magnetic-responsive and pH-responsive characteristics. Moreover, the specific tasks of nanomaterials create opportunity for nanofluids to retrieve those unreachable oil reserves.

Eventually, contrary to the molecular surfactant or polymer stabilized gels, nanoparticle-stabilized gels are very firm even under severe reservoir conditions (Massarweh and Abushaikha, 2021). The main reason for such a capability is its well-organized particle layer at the emulsion interface.

The main objective of the thesis is to simulate the gel treatment process in the core plugs using the Laponite clay HPAM system. Several tasks of the project can be specified as below:

1. Research on EOR methods considering nanogel treatment.
2. To investigate clay-polymer interactions in de-ionized water experimentally.
3. To study the possibility of simulation gel treatment placement in fractured core plugs (IORCoresim).
4. To study the effect of gelation time based on the simulation result.

1.3 Scope of work

This thesis is limited to laboratory bottle tests and simulation to investigate the potential of nanocomposite gels. The work consists of five chapters. Following the introductory chapter 1, Chapter 2 provides a literature review on nanofluids for EOR. The experimental approach, gelation time measurement and simulation of gel placement in fractured core plugs are described in Chapter 3. Chapter 4 provides the results of both experiments and simulation, discussions those results. Finally, Chapter 5 provides a concise conclusion of this study.

Chapter 2 Literature review

2.1 Stages of oil production from a reservoir

Oil recovery from a reservoir is divided into three stages that are: primary, secondary and tertiary recovery (Green, 2018). The first stage is called primary recovery, which means hydrocarbons is being produced through well by the natural energy of the reservoir. In primary recovery, the driving mechanism is liquid and rock expansion drive, gas cap drive, water drive or a combination of these drive forces (Green and Willhite, 1998).

In secondary production, hydrocarbons are displaced towards the oil-producing wells by injecting water, steam or gas (Nolan, 2011). Injected fluids or gas increase the diving force depleted after the primary recovery due to decreased pressure as hydrocarbons are released from the reservoir (Ahmed, 2001). In some cases, even after secondary recovery, almost 80% of hydrocarbons are still in the reservoir (Green, 2018). However, up to 70% of the original oil in place (OOIP) can be produced from high-quality reservoirs (Lake, 1989).

The natural energy of the reservoir depletes with time as the pressure in the reservoir drops with the production of hydrocarbons. Therefore, secondary oil recovery techniques such as gas or water injection injected to maintain the pressure in the reservoir lose their efficiency with decreasing pressure (as the pressure in the reservoir decreases continuously upon production of hydrocarbons). Therefore, pressure is a very important factor to produce hydrocarbons from a reservoir.

2.1.1 Limitations of the secondary oil recovery

As the pressure is finite in the reservoir and the oil production from a reservoir continuously decrease along with the production of hydrocarbons from the reservoir. Secondary oil recovery from a reservoir depends upon the properties of the reservoir and the nature of the reservoir fluid interactions (Jerauld et al., 2008). Mainly secondary oil recovery techniques depend upon pressure building in the reservoir and pushing the hydrocarbons towards the production wells. These techniques are not successful for all the reservoir as secondary oil recovery mainly involves injecting water and gas. However, the water and oil wettability of the reservoir is not altered during the secondary oil recovery, which is the most important factor in pushing the oil towards the production wells. Also, high viscosity makes

the oil immobile or nearly immobile, producing more oil from the reservoir in secondary recovery (Thomas, 2008). Therefore, tertiary recovery or Enhanced Oil Recovery (EOR) methods are used to produce additional hydrocarbons from the reservoir, decreasing the oil's viscosity and altering the water-oil wettability of the reservoir.

2.2 Enhanced Oil Recovery

EOR produces the oil retained in the reservoir due to capillary forces and high viscosity (Thomas, 2008). Therefore, EOR can increase production when oil reservoirs enter the second half of their lives (Joonaki and Ghanaatian, 2014). In the phase of EOR, advanced techniques and processes are applied to produce oil that is still in the reservoir after primary and secondary production. These techniques have proved to increase the production from reservoirs significantly (Thomas, 2008). According to the Norwegian Petroleum Directorate (NPD), about half of the large resources on the Norwegian Continental Shelf (NCS) require EOR techniques (NPD, 2021) which makes EOR very important for the life of an oil field in NCS.

2.2.1 Enhanced oil recovery methods

EOR techniques require an injection of fluids into reservoirs that interact with the Crude Oil- Brine – Rock (COBR) system and simulate the increased production from the reservoir (Green, 2018). These methods raise the reservoir's macroscopic and microscopic sweep (volumetric sweep) efficiency (Stosur et al., 2003). Chemical, miscible injection, forefront, thermal, microbial and CO₂ injection can be considered as the methods of EOR (Vishnyakov et al., 2019) (Figure 2.1). According to EOR can be classified into four different processes (Taber et al., 1997) given as:

- Chemical flooding
- Thermal methods
- Gas injection
- Emerging EOR processes

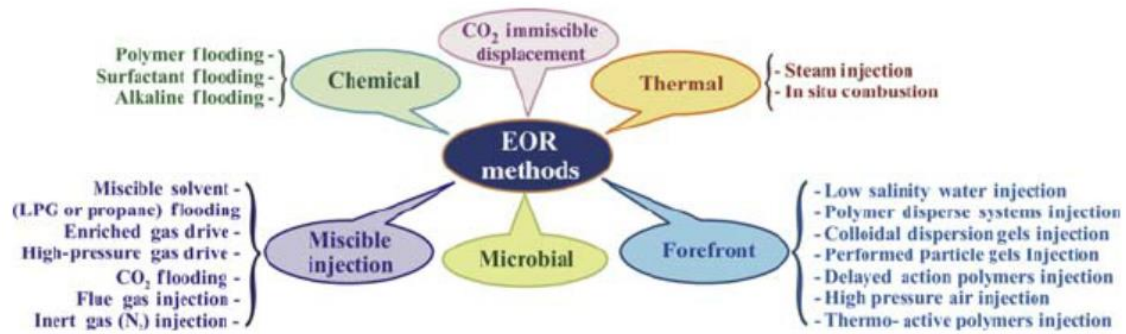


Figure 2.1 Enhanced oil recovery methods (Vishnyakov et al., 2019)

2.2.2 Chemical EOR

Chemical EOR can be divided into three classes:

- Polymer flooding
- Surfactant flooding
- Alkaline flooding

The use of chemical products such as alkalis, polymer surfactants and polymers to increase the oil production is called chemical EOR (Druetta et al., 2019). These dilute caustic and alkaline solutions use chemical formulation to increase capillary numbers (magnitude of viscous forces; viscosity, velocity). It decreases the mobility ratio (mobility of injected fluid, i.e. EOR fluid divided by mobility of fluid displaced, i.e. Hydrocarbons). Thus, chemical EOR is the method that avails to change the properties of water in a reservoir by chemical reactions; it alters reservoir fluid properties and increases oil recovery.

So, water instead of oil can be the dominant fluid in the production stream. Nonetheless, the proportion of water injected into the reservoir interferes with the quality of produced oil (Aronofsky and Ramey, 1956). It leads up to 50% of oil left in the reservoir after water flooding. Adding chemical compounds into the injected fluids causes chemical flooding in the reservoir. It leads to either decrement in interfacial tension between the reservoir oil and the injected fluid or an increase in the viscosity of the injected fluid.

The main idea of polymer flooding is to raise the viscosity of the injected fluid, and high viscous fluid has low mobility. Another process of chemical flooding is used to reduce the

interfacial tension between the reservoir and injected fluid, and it is introduced as alkaline flooding. In addition to that, surfactant without alkaline is also a possible option.

Conventional EOR methods have increased the production of developed oil reserves by up to 50%. However, these methods cannot realize the full potential of the reservoirs (Negin et al., 2017).

The application of nanofluids (in polymer flooding) for EOR has gained significant importance in recent years (Zhou et al., 2020). In addition, injecting nanoparticles is an important technique for EOR to increase production (Youssif et al., 2018).

2.3 Polymer flooding and Rheology

A high oil production rate can be maintained by injecting a large volume of water into the reservoir (Vishnyakov et al., 2019). However, it triggers an increment of the proportion of water in oil production. Therefore, the viscosity of injected water is increased so that amount of water injected into the reservoir can be decreased. To increase the viscosity of the water injected into the reservoir for EOR, polymers are added into water that improves the mobility ratio of the injected fluid (Mohsenatabar Firozjahi and Saghafi, 2020), which results in a better volumetric sweep leading to the accelerated oil production and decreases the proportion of water in the production.

The polymer solution is prepared by adding polymers in water, where a polymer is long-chain molecules having repeated subunits (Vishnyakov et al., 2019). Adding water-soluble polymers in the fluid to be injected for EOR increases the injected fluid's viscosity substantially, resulting in more oil pushing than regular water flooding. Even as small as 0.01-0.1% of polymers addition increases the viscosity of the final polymer solution by 3-4 times. Polymers drive more residual oil from the pore surface as the driving force of injected fluid increases on polymers' addition.

Polymers can be divided into two types, biopolymers and synthetic polymers (Sheng, 2011). Both have their advantages and disadvantages for a specific reservoir and prevailing conditions. It is very important to choose a polymer that has a favorable mobility ratio for the reservoir. Where mobility ratio is the ration of displacing fluid to that of displaces fluid.

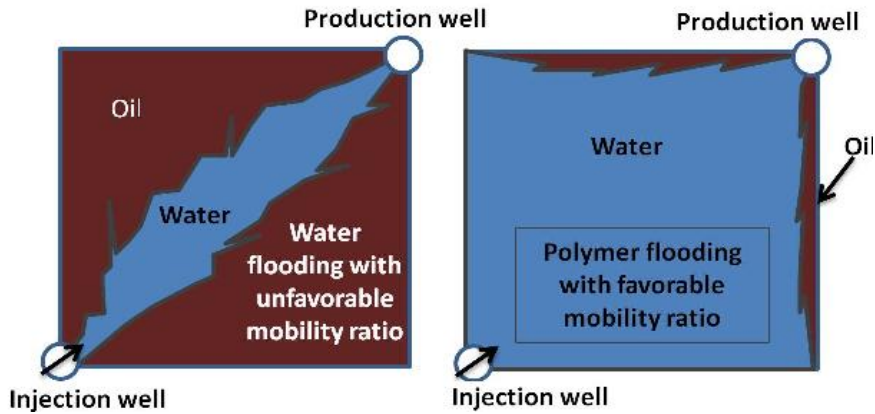


Figure 2.2 Left, using of inappropriate polymer creates fingering effect. Right, using appropriate polymer pushes all the petroleum towards the production well (Zerkhalov, 2015).

Unfavored able fluid may create fingering effect in the reservoir and make it difficult to recover petroleum (Zerkhalov, 2015), as shown in Figure 2.3 below:

The efficiency of polymer flooding depends on the non-Newtonian behavior of polymer

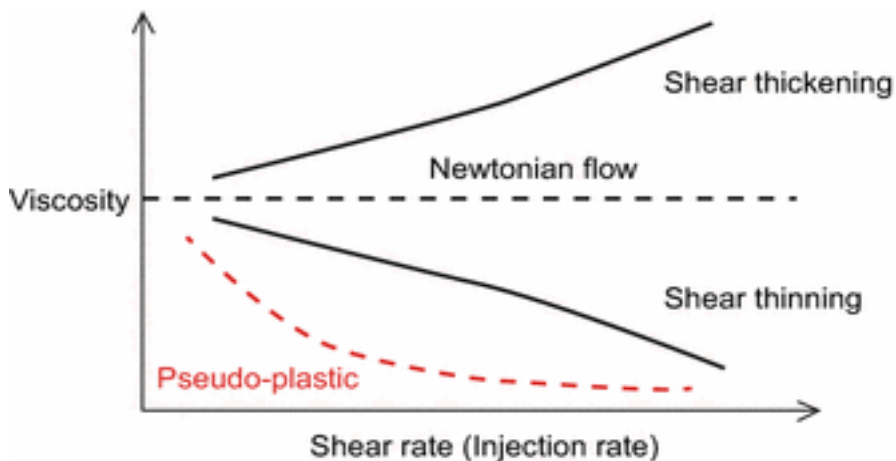


Figure 2.3 Viscosity model of a nonnewtonian fluid (Zerkhalov, 2015).

solution, as shown in Figure 2.3. A non-Newtonian does not follow the laws of viscosity. Therefore, the viscosity of a non-Newtonian polymer solution has non-linear relation with both in-situ shear rate and flow rate (injection rate), as shown in Figure 2.3.

Polymer solutions contain dissolved polymers (e.g., a substance that has been plasticized) or Xanthan biopolymer and partially hydrolysed polyacrylamide (HPAM) (Wever et al., 2011). Owing to its availability and reasonable cost, HPAM is more prevalently utilized in chemical EOR than xanthan biopolymer. When the flux of xanthan or HPAM polymers solution is in the

process, shear-thinning behaviour arises. (Chauveteau, 1981) (Liauh and Liu, 1984); Nevertheless, this behaviour is less observed in HPAM polymer solution (Seright et al., 2010).

Disparate factors like shear rate, degree of hydrolysis, polymer concentration and molecular weight, hardness, salinity and temperature can impact the viscosity of HPAM polymer (Lee et al., 2009). The constriction existing in pores is the main parameter that hastens the presence of shear-thickening behaviour. Therefore, when there is a flow of polymer solution throughout the porous media, the stretching or contraction of polymers chains can be noted, determining the appearance of the viscoelastic behaviour (Koh et al., 2016). The viscoelastic behaviour is always linked to high molecular weight. Thus, near the wellbore zone (where a high shear rate comes across), low molecular weight HPAM polymer solution doesn't exhibit shear-thickening behaviour (Jennings et al., 1971).

Moreover, polymer rheology showed higher deviation from Newtonian behaviour at a high concentration that prevailed at a low shear rate. (Zhu et al., 2021) pointed out at polymer concentration equal to or less than 0.05 wt.%, the polymer viscosity remained constant.

Lately, researchers have been more attracted to show assiduous efforts on studying the potentials of viscoelasticity of HPAM polymer solution to develop displacement efficiency (Wang et al., 2001). They have investigated the impact of the viscoelastic characteristic of polyacrylamide on the decrement of residual oil in "dead ends experimentally" and figured out that the higher the viscoelastic properties, the higher dragging of the remnant oil out of pores will be attained. Consequently, to enhance both volumetric sweep and displacement efficiency, high molecular weight HPAM polymers were applied in field projects. Based on the obtained results, the polymers with shear-thickening behaviour can avail the diversion of fluid into the layer with less permeability and escalate displacement efficiency (Li, 2015) (Banerjee and Tyagi, 2011) (Coste et al., 2000). Despite that, shear-thickening behaviour would crack the formation (near-wellbore zone) and entail the polymer chain's injectivity hardships and striking degradation (Li, 2015). So that, shear-thickening increases as the high molecular weight polymer solution is introduced into the high permeability layers. This behaviour can trigger a microfracture and dwindle the shear stress, and regress polymer to shear-thinning behaviour.

No further test was carried out for higher concentrations of laponite-PEG based gels because of problems with its application in this research (Adijat, 2019). Since the goal of this research was to form a gelant solution which should be easily injectable before it transitions

into a rigid gel in the reservoir, the shear induced gelation property of laponite-PEG solutions will restrict their application for this purpose. The presence of a significant gel structure was observed for higher concentrations of Laponite-HPAM and Laponite-Gellan gum solutions. The strength of the gels formed also appeared to increase with increasing concentration of the Laponite. Laponite-HPAM solutions were also observed to form stronger gels when compared to Laponite-Gellan gum solution. The intercalation of the polymer chains and clay particles to form a rigid gel structure confirm the advantageous effect of the nano-clay and polymer network present in NC gels.

2.4 Functions of nanomaterials in nano-flooding

Recently nanoparticle flooding has received attraction from the industry as a replacement for surfactants and polymers (Kamal et al., 2017) due to their unique properties, which are given below.

2.4.1 Wettability alteration

The tendency of a fluid to spread on a solid surface is called wettability. Wettability alteration is one of the well-known terms for EOR in oil-wet and mix-wet formation, which is defined as the tendency of the surface of the rock or solid for a liquid in the presence of liquids (immiscible) (Wang et al., 2001). This tendency or affinity of rock surface towards the nanoparticles results in occupation of pore spaces by the nanoparticle. In EOR, the wettability of the reservoir rock is changed from oil-wet to water-wet (Mohammed and Babadagli, 2015). This process pushes the oil in the reservoir towards the production well.

The oil trapped in the reservoir for millions of years before recovery processes were started, reservoirs usually show oil-wet or mix-wet formations because of long-term surface contact between formation and oil reserve (Peng et al., 2017). Changing formation wettability will end up with an increment in the mobility of the oil phase as capillary force decreases. Many studies have been carried out to emerge the general mechanism of wettability alteration in different kinds of literature. There are two common explanations of general mechanism. It is either surfactant absorbing on rock surfaces changes wettability or natural lyophilic surfactant generated by crude oil oxidization removed by ion pairs. Considering the effects of

nanoparticles on wettability alteration, much research was reported by Giraldo and Maghzi (2013). They found that particle size, co-surfactant, pH value and ion strength can alter the wettability of formation (Peng et al., 2017)

If the medium is oil-wet, the waters are trapped inside the pores, and the oil remains attached to the wall of the reservoir rock, as is shown in Figure 2.4. Therefore, it can be observed in Figure 2.4 that oil (darker material) is in contact with the particle. However, nanoparticles break the bond between the oil and surface of the reservoir, increase the water wetness increasing the production of oil (Maghzi et al., 2011) as shown in Figure 2.4 that water (light coloured) is in contact with rock particles.

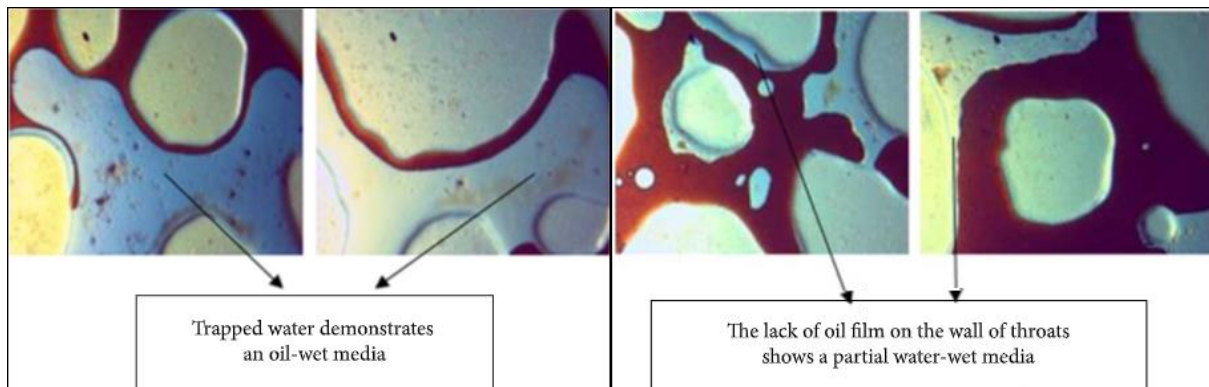


Figure 2.4 Showing oil wettability of the reservoir (left). Increase in water wettability after injection of EOR fluids (Maghzi et al., 2011).

2.4.2 Reduction of IFT

To increase the oil recovery ratio, it is very common to reduce IFT between oil and water (Arekhov et al., 2020). IFT (as a standard parameter) is used for surfactant characterization for chemical flooding. From the literature, it is well-known that the lowest oil-water IFT by molecule surfactant is between 10^{-2} and 10^{-3} m N/m. However, such small interfacial values cannot be achieved in nanofluids system, development of nanomaterials comes out as a discussible topic by researchers. Using hydrophobic and hydrophilic characterization of nanoparticles, Gennes created a particle called Janus particle. Janus particle can reduce IFT (Peng et al., 2017), resulting in increased oil recovery from the reservoir.

2.4.3 Controllable viscosity

The ratio between the displacing and displaced is called the mobility ratio (Peng et al., 2017). A high mobility ratio with higher sweep efficiency and more negligible fingering effect in the reservoir is desired for more efficient oil displacement. Nanofluid is commonly used to increase displacing fluid viscosity, and it tends to reduce oil viscosity. High displacing fluid viscosity and lower oil viscosity causes a boost in oil production (Peng et al., 2017). If the viscosity of the injected fluid is increased, it will, in turn, increase the oil displacement efficiency (Khan et al., 2018).

The use of nanoparticles can significantly lower the interfacial tension, increase water wettability of the reservoir, and improve the rheological properties, increasing the oil production from a reservoir (Mohammed and Babadagli, 2015). Experiments have shown that the use of nanomaterials increases oil recovery between 35 – 50 per cent inhomogeneous pore medium (Suleimanov et al., 2011).

2.4.4 Factors controlling the success of Nano flooding

The application of nanotechnology is an advanced method for EOR operation. The assessment of nanomaterials is an important process determining if they satisfy the criteria to implement EOR without damaging the reservoir (Peng et al., 2017). Nanomaterial structure, morphology and surface modification formation salinity, temperature and pH value can affect nano flooding quality.

2.5 Morphology of nanoparticle.

The morphology of nanofluids is the main concern for EOR operation. The scale difference between nanoparticle size and pore size is an important criterion for successful nanofluid operation (Peng et al., 2017). A possible physical limitation in nanofluids can be the size of the pore throat compared to nanoparticle size. Formation damage will happen if the nano particles' size is greater than the size of pore throats.

Aggregation of nanoparticles is the formation and growth of clusters controlled by particle chemical transport, and interfacial chemical reactions can also cause blocking of pores even

though the individual nanoparticles are much smaller than the pore in Figure 2.5 (Al-Hajri et al., 2018)

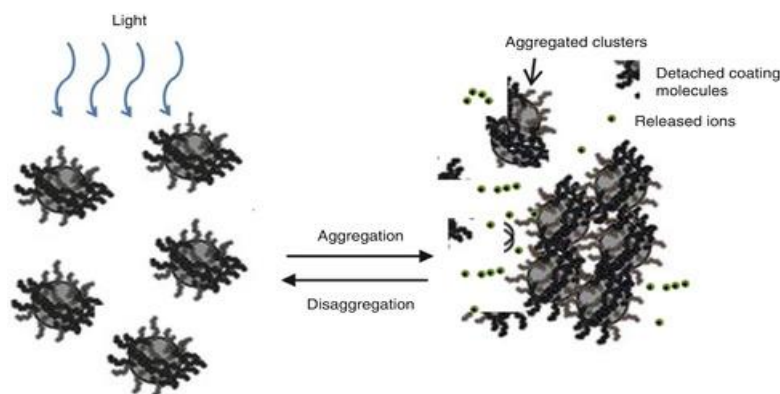


Figure 2.5 Mechanism of Aggregation in nanoparticles (Al-Hajri et al., 2018)

Oil emulsification is also influenced by the shape and morphology of the nanoparticle (Peng et al., 2017). Therefore, the shape of nanoparticle also plays an important role in surface coverage.

2.6 Polymer gels

A huge amount of water production often accompanies oil and gas production from the reservoirs (Kantzas et al., 1999). Excessive water production from the oil and gas reservoirs is one of the major problems faced by the petroleum industries worldwide. Gels have been successfully used for many years to control water production. The Polymer-solvent system is the base of polymer gels (Banerjee and Tyagi 2011). This system holds a large amount of solvent by a three-dimensional network which consists of polymers and aggregates. Polymer gels can be categorized into two types: physical and chemical gels. Physical gels are classified because of intermolecular association by van der Waals, electrostatic and hydrogen-bonding interactions. Chemical gels are a combination of polymer network which cross-linked in a large amount of solvent. In the point of thermal reversibility, chemical gels are thermally irreversible as being different from physical gels.

2.6.1 In-situ Gel (Traditional method)

Several chemical materials such as polymers, crosslinkers, and additives can be combined and create cross-linked polymer known as in-situ gels (Temizel et al., 2016). Two adjoining polymer molecules are connected chemically and physically by the cross-linking agent. The liquid form of this composition is called a gelant. The gelant in an in-situ system is injected into the formation and the gel forms under reservoir conditions. The generation of the gel depends on the various condition in the reservoir, such as increasing temperature and pH alteration. Gel strength is controlled by changing the gelants composition and surrounding condition. From Figure 2.6, it is obvious that the strength of gel can be classified as either weak or very strong (Imqam, 2015).

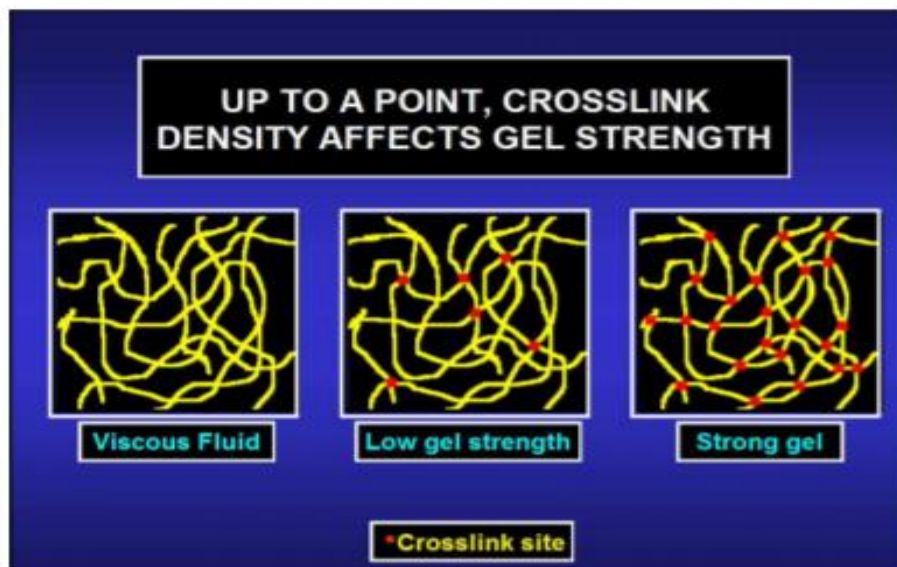


Figure 2.6 Gel composition (Imqam, 2015)

2.6.2 Preformed gel systems

Preformed gels are generated in the surface facilities and inject into the formation afterwards (Seright, 1997). In a reservoir condition, we do not observe the gelation process. Using this kind of gel, the preformed gel can solve the problem related to the in-situ gel system. The problems are described as below:

1. Dilution of formation water, the adsorption and chromatography of chemical composition and shear by pump, wellbore, porous media dwindle the cross-linked reactions of gel.
2. Some damages on the inefficient low permeable zone.

Preformed gels are classified in Figure 2.7 by their particle size, developer, applications swelling ratio and swelling time (Imqam, 2015).

Name	Developer	Particle Size	Applications
Bright Water®	Chevron, BP and Nalco	Sub-Micro (< 1 µm)	60+ injectors
Microgel	IFP	Micro (1-10 µm)	10+ producers
PPG	PetroChina, MS&T, and Halliburton	Millimeter (10 µm to millimeters)	5,000+ Injectors in China
pH Sensitive polymer	UT	Micro	Not reported

Figure 2.7 A summary of preformed gel systems (Imqam, 2015)

2.6.3 Bright water

Bright water is one type of systems developed by BP, Nalco, and Chevron. Bright water, significantly small particle size (0.5 mikron), is injected with injection water in the reservoir (Roussennac and Toschi, 2010). As the particle's sizes are significantly small, it allows the particles to propagate through the rock's pores with the injected water. While it passes through the reservoir, the polymer gradually warms toward the reservoir temperature. As a result, it swallows its original volume many times, blocking pore throats in Figure 2.8. Various parameters such as salinity, reservoir temperature and targeted thief zone properties affect the ability of bright water particles.

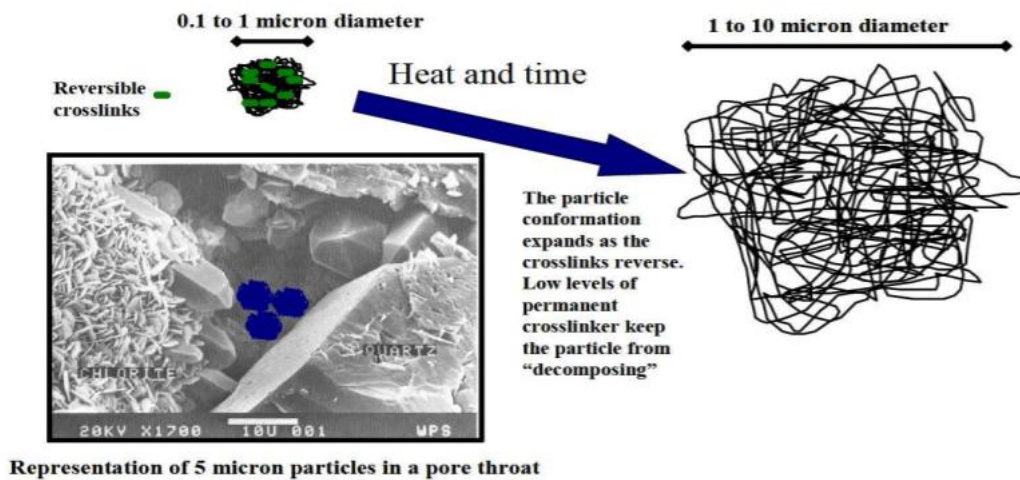


Figure 2.8 Mode of activation of the particulate reagent (Imqam, 2015)

2.6.4 Microgel

The cross-linked polybutadiene particle latex can be the base of the microgel, which named after considering the size of the particle (less than 1000 nm) in Figure 2.9 (Yuan et al., 2019). Microgel can swell easily in an organic solvent. Microgels are dispersed in a solvent, and this solvent helps it to swollen. Molecular forces such as covalent or strong physical force act as a stabilizer to hold polymer network in microgel. The main use of microgel is water shut off and conformance control operations (Imqam, 2015). The following parameters classify the microgel:

- The particle size of the microgel is in the range of 10-1000 nm.
- The microgel can disperse in a solvent. Thus it leads to swelling in microgels.
- With the help of strong physical forces in microgel, make a covalent and stable structure.

The water-soluble, non-toxic, soft, stable, and size-controlled microgels injection method was developed (Chauveteau et al., 2003). It is shown that microgels can easily adsorb rock pore surfaces in rocks, forming soft monolayers with a thickness equal to their size. Consequently, water permeability can be controlled by adjusting this thickness during

the manufacturing process. This study represents the utilization possibility of such microgels for water shutoff (WSO) treatments.

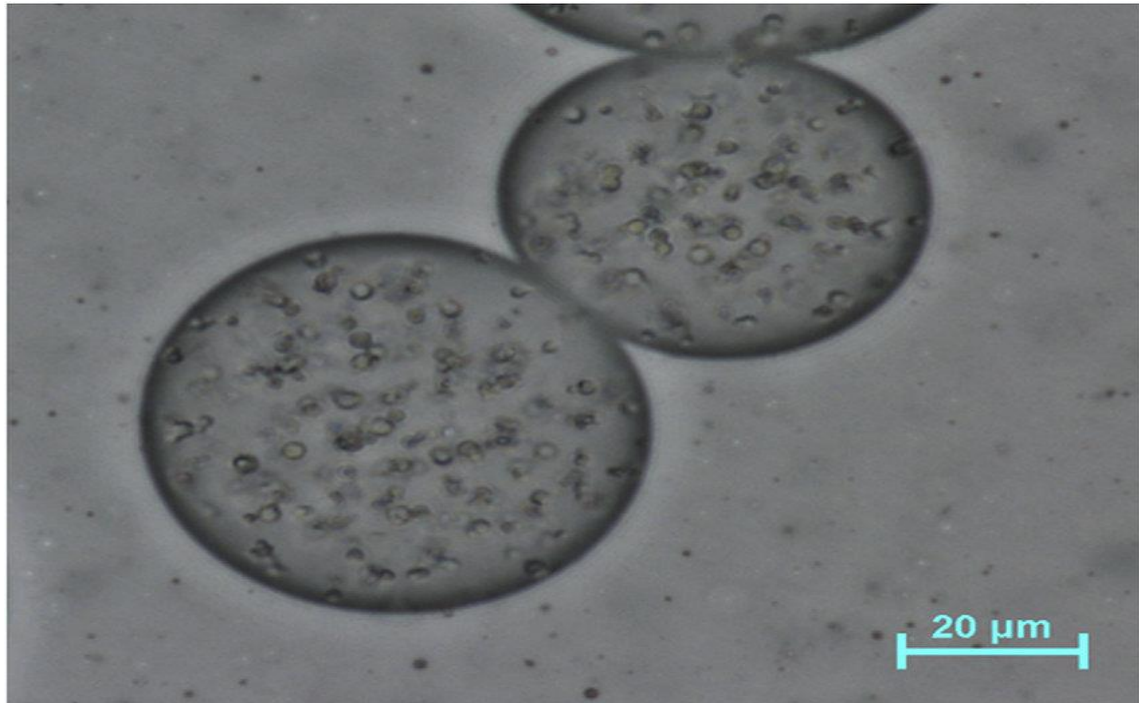


Figure 2.9 Microgel particles (van der Schaaf et al., 2016)

2.6.5 Preformed particle gel (PPG)

The characteristic of PPG is the same as a preformed gel (Sun et al., 2020). Gelation happens in the surface facility before injecting it into a reservoir in the PPG system, which means there is no gelation process in the reservoir. PPG gels are one of the super sorbent polymers which have different behaviour from unswollen in-situ gels. It has a high absorption ability, which can absorb a large quantity of fluid in an aquifer. Some experiment in Figure 2.10 clarified that PPG could absorb many fluids, and it is not easy to discharge absorbed fluid (Imqam, 2015).

Particle size in PPG gel can be adjustable on a scale of micrometres and millimetres. Particles swelling ratio varies from 30 to 200 times of original volume. The concentration of brine solution is used to control the particle size (Imqam et al., 2017).

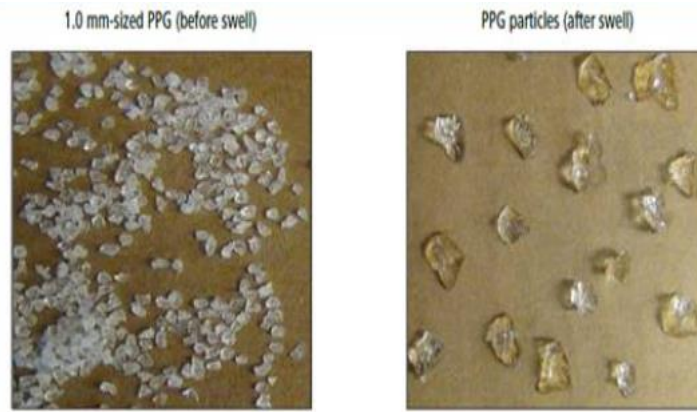


Figure 2.10 PPG particle before and after swell (Imqam et al., 2017)

2.6.6 pH-sensitive polymer

pH-sensitive polymers were used in the (Al-Anazi and Sharma, 2002) experiment as a conformance controller. The sensitivity of polyelectrolytes is observed, and pH, ionic change and polymer concentration are considered the leading cause of this sensitivity. For example, pH-sensitive polymer shrinks to a low viscosity case of acid possibility in the reservoir. As well as swelling and adsorbing water are observed when pH increases. The chemistry theory of the swelling process in the gel was explained by (Al-Anazi and Sharma, 2002) (Figure 2.11). In the chemical process in the polymer chain of polyacrylic acid, ions interact with the hydroxyl group; this electrostatic repulsion force causes the polymer to uncoil. This procedure causes viscosity increment.

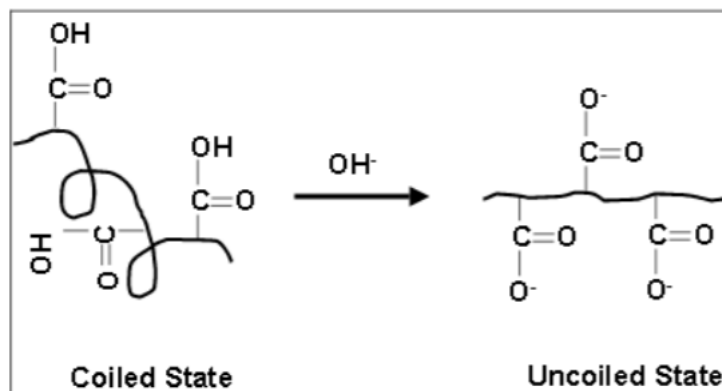


Figure 2.11 Swelling of Polyacrylic acid swelling within ionization (Al-Anazi and Sharma, 2002)

2.7 Simulation of gelation and gel placement

There is a study about the simulation of gelation (Yuan et al., 2000a). Therefore, two simulations are possible to carry out considering the two types of gel treatment: near-wellbore and in-depth gel treatments.

In-depth gel treatment injects gel deep into high permeability layers and diverts the subsequent water flow into lower permeability layers (Tsau et al., 1985).

Regarding heterogeneity of reservoir and high-water production in petroleum fields, wellbore gel treatment is used to plug the large pores of these formations to reduce permeability. Thus, it is a remedial method applied for conditioning high permeability formations and prevents undesirable problems that cause a high cost to the oil industry (Scott et al., 1987).

Instead of laboratory test, which is a costly procedure and has limited capacity, simulation methods are used to research the gelation process. (Khamees, Flori, and Wei, 2017). One of the studies on the simulation of in-depth gel treatment is carried out by Khamees. They used commercial “CMG-STARS “simulator to demonstrate the effectiveness of in-depth gel treatment in correcting the heterogeneity in a thick reservoir. The model consists of one injector and three producers with three layers of different permeabilities and thicknesses. This research concluded that injecting low PV (pro-vesicular) of gel into high permeability layers of the reservoir could raise the oil productivity. In addition, he studied to reveal the effects of gel degradation on reservoir performance by using three scenarios: no degradation, two years, and four years degradation. The results showed that the runs without degradation yielded a higher recovery factor regardless of the injected PV. When the gelant was injected into only high permeability layers, higher incremental oil and higher oil recovery factors were obtained than runs when the gel is injected into all three layers. Moreover, the more homogeneous the reservoir is, the higher the recovery factor could be obtained. The appropriate time for gel injection is investigated too. It was found out that the best time to start gel treatment is when the water cuts are higher than 80% because of the recoverable oil content in high permeable layers before that time. Other tests were run to discover the importance of injecting gel and polymer together. When the gel was injected into all three layers with four years of gel degradation and two years of polymer degradation, the results showed that polymer flooding followed by gel treatments produced better results than gel treatment followed by polymer flooding (Yuan et al., 2000a).

Two principal factors responsible for the low sweep efficiency are the heterogeneity of reservoir and improper mobility ratio of displacement (Mack and Smith, 1994). An in-depth fluid diversion technique deploying low concentration flowing gel (LCFG) is an attractive method for altering reservoir heterogeneity and enhancing the mobility ratio of displacement. LCFG serves as both a flooding and plugging agent, considering its capability to flow in the porous media. The limitation of the near-wellbore treatment by high concentration squeezing is surpassed since the LCFG can penetrate deeply in the reservoir, especially when a large LCFG is injected. Consequently, a successful rate in the test was acquired relative to near-wellbore treatment (Fielding et al., 1994). Low-concentration polyacrylamide with cross-linking agent forms the LCFG. The expense could have dwindled considering the amount of polymer deployed is just one to two-thirds of that conventional method. It showed very promising potential for future application. (Han et al., 1998).

However, in several numerical simulation studies, the behaviour of the LCFG was still described as a near-wellbore treatment or flooding agent. Because the features and physicochemical properties of the LCFG were not taken into account in these numerical simulation studies, the substantial deviation could be the consequence. (Yuan et al., 2000b). These neglected properties are LCFG formation, character, and permeability reduction, principally the mobility in the reservoir. Therefore, a numerical simulator with 3D, 3 phases and nine components was constructed. It possessed the function of stimulating LCFG injection, in-depth profile modification, chemical gel near-wellbore treatment, polymer flooding, and conventional water flooding (Yuan et al., 2000c). The effects of polymer concentration, the gelation time, the kinetic of reaction on the formation of LCFG, the influence of transition pressure of LCFG on the mobility of LCFG in porous media and the effects of viscosity and permeability reduction on the plugging function were taken into account in this model. (Khamees et al., 2017). Polymer flooding technique is applied commercially with great success in numerous oilfields of China, and the average increased recovery is approximately 13.7%. In some critically heterogeneous reservoirs, oil recovery can be enhanced more by LCFG injection than polymer flooding. Furthermore, LCFG injection can be used to develop recovery further in polymer flooded reservoirs. In the pilot area, the recovery of the reservoir was increased up to 51% by polymer flooding. So, 49% OIP remained in the reservoir; an LCFG injection pilot test was developed to sweep further efficiency and ultimate recovery (Yuan et al., 2000b). Numerical simulation analysis by using the simulator POL-GEL was implemented for both pilot design and LCFG injection mechanism survey. POL-GEL is a simulator with 3-

dimension, 3-phase (oil/gas/water), 9-component (oil/gas/water/polymer/crosslinker/gel/univalent/divalent/additional sensitive component) (Khamees et al., 2017).

The procedure of simulation studies is as below:

1. The simulation study and history match of water flooding, polymer flooding and LCFG injection were conducted to verify the simulator (POL-GEL) and formulate parameters for field application.
2. The history match of the polymer flooding within the test area was studied to understand the initial condition.
3. The numerical simulation study of LCFG injection was conducted to predict the scope of EOR and evaluate the economic efficiency.

The simulator POL-GEL is created to possess the basic functions of general models. Still, it can also be utilized to simulate all types of gelling polymers that have lately evolved. The model considered the essential mechanism, basic physicochemical phenomena, and influencing factors of gelling polymers. Apart from polymer flooding and profile alteration by gelling polymer, which is primarily concerned with gel formation, the model also includes permeability reduction and flowing capacity. Thus, it can be used for water flooding simulation and prediction, polymer flooding, near-wellbore treatment and in-depth fluid diversion of LCFG with high or low concentration polymer. This simulator has been tested in the lab and the field, and it has a high stimulation capacity and flexibility in terms of deployment (Han et al., 1998).

2.8 Laponite clay

Laponite is a silicate synthetic clay mono-dispersed with a disk of diameter ranging from 25-30 nm with a thickness of 0.92 nm (Kroon et al., 1996). One octahedral magnesia layer in two tetrahedral silica layers on each side forms a Laponite disk. Some of the magnesium ions substitute isomorphically by lithium ions can pose a minimum positive charge in the octahedral layer (Shahin and Joshi, 2012). The other faces of a particle having extra electrons share with the sodium atoms. The sodium atoms stay between the disk as Laponite disks in stacks (Joshi, 2007). Laponite disks swell in aqueous media in case of water existences. It causes the disassociation of Na^+ ions that comes from stacks due to the osmotic gradient. Disassociation of Na^+ ions leads the Laponite particles to a negative charge (Tiwari et al., 2014). MgO and

MgOH form the edge of laponite particle as broken crystals. This process obtains a positive charge at low pH and a negative charge at high pH (Lin et al., 2021). Van der Waals force is observed between Laponite particles. The ionic concentration of Laponite particles increases in the presence of salt, which can be considered as obstacles for charges on particles while affecting the electrostatic interactions among particles in the same way. Watery suspension of Laponite has been a well-known research area considering complex inter-particle interactions. Various characterisation methods have been used to find out a microstructure of aqueous suspension of Laponite. Light scattering (Cummins, 2007), x-ray scattering (Ruzicka et al., 2011), micro rheology (Pujari et al., 2011), rheology (Mourchid et al., 1998), visual observation (Ruzicka et al., 2011), microscopy (Pujala, 2014), and simulations (Rich et al., 2011) is utilized by a function of Laponite concentration (C_L) and salt concentrations (C_s).

Over the last two decades, various phase diagrams have been proposed, modified, and re-proposed. It is observed that for $C_L < 1$ weight %, suspension undergoes phase separation. Laponite suspension, above a concentration of 1 weight %, often undergoes a phase transition from a free-flowing liquid to a soft solid over hours to months, depending on C_L and C_s (Ruzicka et al., 2011). Laponite suspension flows from the liquid phase to a soft solid within hours or months; it depends on Laponite and salt concentration. The average time for phase transition for soft solid is smaller at higher values of C_L or C_s in Laponite suspensions. This soft solid forming resulted in a gel by linking the negative faces and the positive edges with a concentration range between one and two-weight %. No microstructure create a soft solid-like state at a concentration of Laponite suspension above 2 weight % (Ruzicka et al., 2011). One study represents that Laponite particles act as repulsive glass at this concentration regime; particles remain reserved; thus, there is no collide within neighbour particles due to the repulsion among the negative charge faces. Opposite to the above proposal, other studies show gel formation with edge to face bonds, leading to a fractal network. According to some investigations, Laponite suspension systems can behave either repulsive glass or attractive gel state at the Laponite concentration rate of 1.8- 2 weight % (Mongondry et al., 2005).

Chapter 3 Experimental and simulation methods

Experimental procedure and materials used in this thesis are presented in this chapter. The experiments were carried out to investigate clay-polymer interactions in de-ionized water.

3.1 Chemicals

Polymer and clay are used as primary chemicals for creating gel considering gel components' molecular and chemical structure (Rezazadeh et al., 2020).

3.1.1 Polymer

Hydrolysed polyacrylamide (HPAM) was selected for investigation in this research because of its popular use in polymer gels (Seright and Brattekas, 2021). HPAM (Flopam 3630) of high-molecular-weight 18,000,000 Daltons from SNF S.A.S was used (Wehle, 2013).

3.1.2 Clay

Laponite RD (from Alfa Aesar) with the composition $\text{Na}_{+0.7} [(\text{Si}_8 \text{Mg}_{5.5} \text{Li}_{0.3}) \text{O}_{20}(\text{OH})_4]^{-0.7}$ is a synthetic layered silicate clay with an average lamellar structure diameter of 25nm and average lamellar thickness of 1nm (Shahin and Joshi, 2012).

3.2 Equipment/Materials

The experimental procedure and materials used are listed below:

1. Magnetic stirrer: Heidolph MR hei-standard stirrer was used for mixing solutions
2. Vortex Shaker: For mixing test tube gel solutions
3. Oven: For heating gelant solutions at 50°C
4. Weighing balance: A Mettler Toledo PB303 balance was used to measure all chemicals and solutions
5. Test tube/conical flask: For storing NC gels

3.3 Characterisation of Laponite-HPAM interactions

Clay-polymer interactions in de-ionized water are examined. This procedure was implemented by examining laponite-polymer interactions. The results from different tests are then compared and, the most promising gel composition is selected.

3.4 Examination of Laponite-polymer gelation properties

This section presents the examination of laponite clay interaction with the different concentration of polymers. The experimental procedure is described below.

- Polymer solutions:

Bulk polymer solutions were prepared and then diluted to desired concentrations. For example, bulk polymer solutions of 0.03 wt% and 0.3 wt% were prepared by adding powdered polymer to deionized water. When preparing the lower concentration (0.03 wt%), 0.03g of polymer was added to 99.97g of deionized water while mixing with a magnetic stirrer for 2 hours. Conversely, for the higher concentration, 0.3 g of polymer was added to 99.7g of de-ionized water while mixing with a magnetic stirrer for 2hours.

- Laponite dispersions:

Various concentrations of laponite dispersions were investigated. However, the method of preparation remained the same, (a) desired amount of clay was measured, (b) clay was added into a pre-measured amount of deionized water while mixing with a magnetic stirrer, (c) Dispersion was mixed until a clear homogenous dispersion was obtained. It is essential to mention that due to the ageing of laponite dispersions, the dispersions were prepared a few minutes before their use

- Nanocomposite gel preparation:

The steps for preparing nanocomposite gels are described as follows: (a) desired quantity of polymer was measured and placed into a test tube, (b) desired quantity of clay solution was then measured and added to polymer solution from 'a', (c) solution from 'be was then mixed with a vortex mixer at speed 7 for about 1min.

- Gel characterisation:

Screening and characterisation of prepared nanocomposite gels were carried out by simple inversion or/and shaking of the tubes with a vortex mixer at speed 1 for 30secs and then visually inspecting gel status. Gels are then characterized based on the gel code described in Figure 4.1.

3.5 Simulation Part

We present a simulation of produced water for the core plug, compared with data, gel injection in a core. The simulator IORCoreSim is used to investigate gelation with different Laponite clay and HPAM concentrations, injection time, gel location and their effect on recovery. IORSim modifies the reservoir permeability due to the gelling, and the macroscopic sweep is improved.

3.5.1 IORCORESIM: Mathematical Model

All simulations were run using IORCoreSim, a development of BugSim (Lohne et al., 2019). IORCoreSim is a core scale simulator developed at the IOR Centre of Norway, aimed to handle SCAL and EOR experiments (Lohne et al., 2017) and help upscale EOR processes from lab to field. The main flow field is obtained from a finite-difference discretization, using a sequential solution method for pressures and saturations. First, the oleic pressure field for the new time level is calculated from the linearized pressure equation, keeping the saturation-dependent variables fixed at their values from the previous timestep. Subsequently, the new saturation field is found by solving an additional saturation equation formulated in terms of the fractional flow of water. The fractional flow equation is solved implicitly with respect to the saturation dependent variables k_r (relative permeability) and P_c (capillary pressure), while keeping the oleic pressure and total flow rate from the pressure solution fixed. Phase velocities obtained from the new saturation solution are then used to compute component transport velocities. The latter is not necessary if only two components, one aqueous and one oleic, are defined.

3.5.2 Simulation Input

The main input parameters required to run the simulator are

- Core dimensions and properties (diameter, length, porosity, permeability)
- Fluid properties (viscosity, density, oil/water IFT)
- Gel properties (modelled in terms of compressibility, porosity, permeability)
- Saturation functions (relative permeability, capillary pressure)
- Boundary conditions (pressure, contacting fluid)

3.5.3 Grid Description

The 3D grid is a simple corner point geometrical grid with a dimension of 240 x 31 x 7 grid blocks, dx, dy and dz. Individual sizes for all blocks are $n_x=0.03$ cm in x -direction, $n_y=0.11$ cm in y -direction and $n_z=0.48$ cm in z -direction, Figure 3.1.

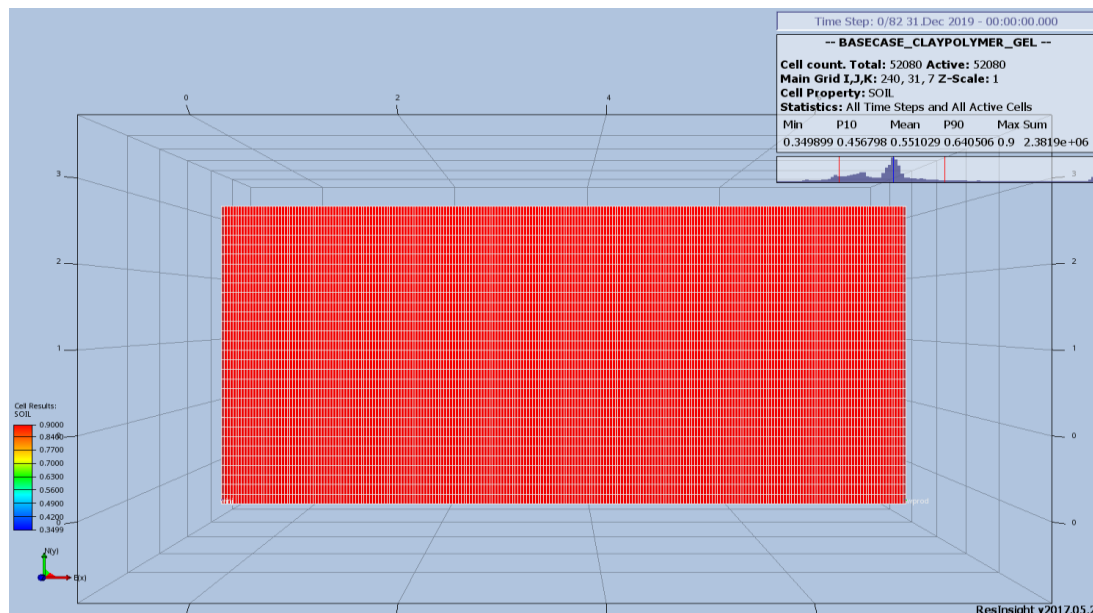


Figure 3.1 Core view from the top

3.5.4 Well Information

This part gives an overview of the information of the wells. First, two vertical wells are drilled: injection well and production well with (11;16;4) and (230;16;4) coordinates, respectively, Figure 3.2.

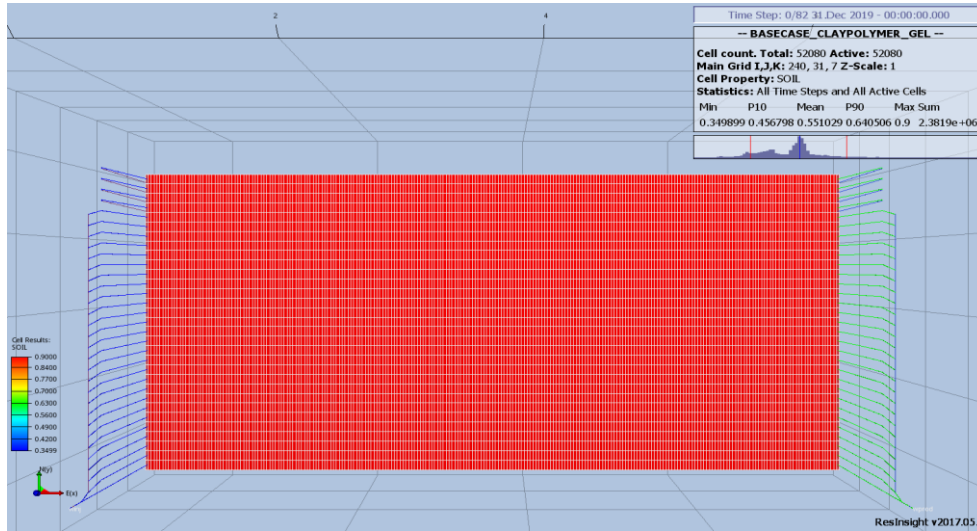


Figure 3.2 View of wells from top

3.6 Gel time calculation

The gelation time is the amount of time it takes for the plastic encapsulant in the liquid form to transform into a gel (Ardebili et al., 2019). The encapsulant in the gel form is a highly viscous material that can no longer flow or be smeared into a thin coating.

The gelation rate is calculated as below (Lohne, 2020):

$$\frac{dc_g}{dt} = r_g C_1^{\alpha_1} \exp\left(\sum_{i=2}^{n_{gv}} \alpha_i C_i^{\beta_i} + \frac{E_{ag}}{R} \left(\frac{1}{T_{ref}} - \frac{1}{T}\right)\right) \quad (1.1)$$

$$\frac{dc_g}{dt} = -Y_{g1} \frac{dC_1}{dt}$$

C_1 represents the main component being converted to gel, r_g is the correlation coefficient for gelation rate, and the temperature T is in °K and $R=0.008314$ kJ/(K·mol). To compare with

laboratory measurements, Eq. (1.1) can be integrated to give the gelation time, which in the model is the time when a critical gel concentration C_{gcr} is reached.

$$t_{gel} = \frac{C_{1,0}^{1-\alpha_1}}{k(1-\alpha_1)} \left(1 - \left(1 - \frac{C_{gcr}}{Y_{g,1}C_{1,0}} \right)^{1-\alpha_1} \right) \quad (1.2)$$

$$k = r_g \exp \left(\sum_{i=2}^{n_{gv}} \alpha_i C_i^{\beta_i} + \frac{E_{ag}}{R} \left(\frac{1}{T_{ref}} - \frac{1}{T} \right) \right) \quad (1.3)$$

All gel above this critical concentration is irreversibly retained and denoted adsorbed gel, A_g .

In this case, the parameters are adjusted to a gelation system where units wt.% was used for gel, clay and polymer and mg/l for Ca concentration. In IORCoreSim, the wt.% unit is approximated with g/100 ml. Taking the adjustment into account in Eq. (1.2), gelation time is calculated as:

$$t_{gel} = \frac{C_{clay}^{(1-\alpha_{clay})}}{k(1-\alpha_{clay})} \left(1 - \left(1 - \frac{C_{cr}}{C_{clay}} \right)^{1-\alpha_{clay}} \right) \quad (1.4)$$

$$k = r_g \exp \left[\alpha_{polymer} C_{polymer}^{\beta_{polymer}} + \alpha_{Ca} C_{Ca}^{\beta_{Ca}} + \alpha_{clay} C_{clay}^{\beta_{clay}} + \frac{E_a}{R} \left(\frac{1}{T_{ref}} - \frac{1}{T} \right) \right] \quad (1.5)$$

k is reaction rate (Lohne, 2020).

Chapter 4 Result and Discussion

This chapter presents the results acquired during the experiment and simulation.

4.1 Experiments

To properly monitor the gelation mechanism and describe the characteristics of the gels formed. A gel code based on a literature study (Skrettingland et al., 2014) is provided below in Figure 4.1

Gel Code	Gelant status upon gentle shakes/inversion of tubes
1	Seems to have original viscosity (no gel)
2	some increase in viscosity (freely flowing gel)
3	Highly viscous and deformable flowing fluid
4	Deformable upper part with high flow resistance
5	Rigid gel (no flow or deformation)

Figure 4.1 Characterisation of gel code (Skrettingland et al., 2014)

4.1.1 Characterisation of laponite gels in Deionized water

Different types of behaviours were observed upon the preparation of gelant solutions with the selected types of clay and polymers at different concentrations. Table 4.1 presents the various laponite and clay gel combinations investigated and their respective concentrations. After the experiments, we observed visually all gelants and considering Figure 4.1, gel code was selected. Gel codes were obtained for the 1st, 3rd and 4th experiments after one day; gel code for the 2nd experiment was applied after two days.

Table 4.1 Investigation of Laponite-HPAM interactions in deionized water, heated at 50°C.

	Clay	Concentration (wt%)	Polymer	Concentration (wt%)	Gel code
1.	Laponite RD	2	HPAM	0.3	4
2.	Laponite RD	1	HPAM	0.3	4
3.	Laponite RD	1	HPAM	0.03	3
4.	Laponite RD (Adijat 2019)	1.5	HPAM	0.3	5

4.2 Gelation time

Gelation time for gels with various clay-polymer interactions was calculated considering input parameters of the gel model (Table 4.2) and gel components (Table 4.3).

Tuning was carried out to relate existing parameters for gelation time calculation to experiments.

Table 4.2 Gel Model

Parameters and units	
E_a , kJ/mol	77
T_0 , °C	323.15
$C_{critical}$, %	0.15
E_a/R	9261.487
R_g , 1/day	6.58E-03

Table 4.3 Gel components

Name	α	β
LP Clay	1.5	0
HPAM	0.7	1

With the help of equation 1.4 and 1.5, gelation time was calculated in Table 4.4. The reaction rate is calculated and inserted into the formula for finding gelation time. The effect of the calculated reaction rate can be seen below:

Table 4.4 Gelation time

Laponite clay, %	Polymer, %	Temp °C	rg,1/day	C _{critical} , %	k	Gelation time, hours
1	0.3	50	6.58E-03	0.3	8.12E-03	48.1
1.5	0.3	50	6.58E-03	0.3	8.12E-03	23.7
2	0.3	50	6.58E-03	0.3	8.12E-03	14.7
1	0.03	50	6.58E-03	0.3	8.12E-03	10.3

4.3 Simulations

There are overall 7 cases simulated to observe how the gelation effects change oil recovery in reservoirs. All those observations provide us with the answer to the questions: How would the gelation process in the reservoir positively impact oil recovery?

To present each data from the result of simulations will be as below:

- Production rate versus pore volume.
- Pressure drop versus pore volume.
- Gel components concentration versus pore volume.
- Oil recovery versus pore volume.

4.3.1 Base case

We chose to inject fluid containing Laponite clay with 2 % and HPAM polymer 0.3% concentration at a 2 ml/h flow rate within 5 hours in the Base case. Gel components injection carried out at between 0.48 and 0.88 pore volume; then water injection started again from 0.88 pore volume Figure 4.2. Therefore, the shut-in period was started to be processed in 0.88 pore volume, 24 hours.

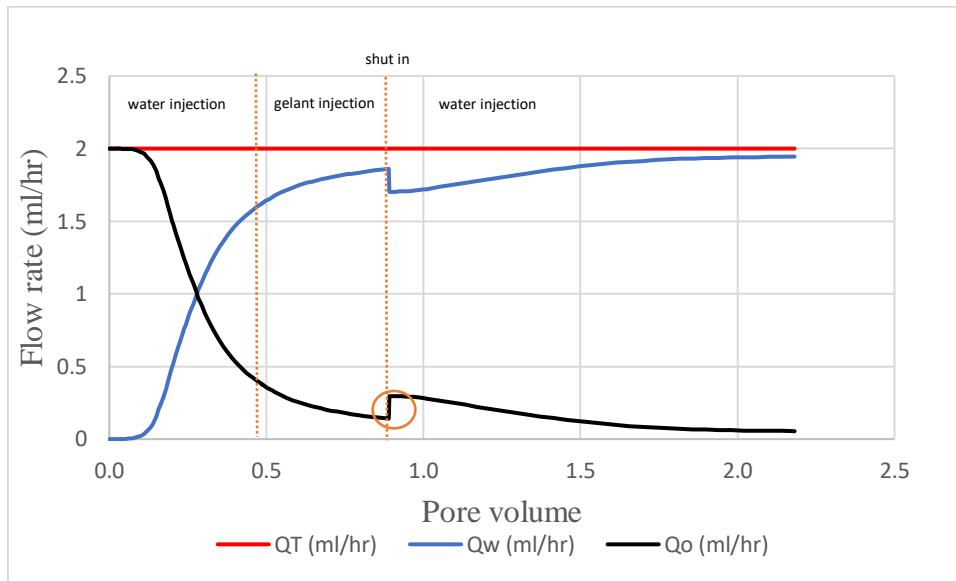


Figure 4.2 Production rates for the Base case

From Figure 4.2, the effect of gelation can be observed at around 0.9 pore volume with raising in oil and decreasing in water production, respectively. Thus, injection of gel components is enough to create gel flooding in the reservoir where oil production can increase.

The proportion of gel components in production is observed as in Figure 4.3. Production of gel components are almost at the same initiation time of injection with a slight delay, but this time is enough to have gelation process in core Figure 4.3.

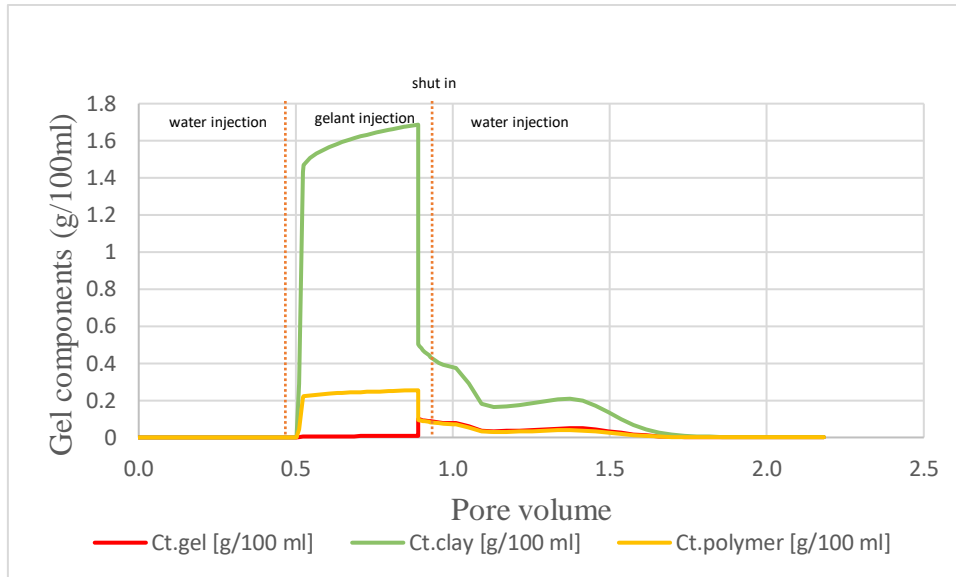
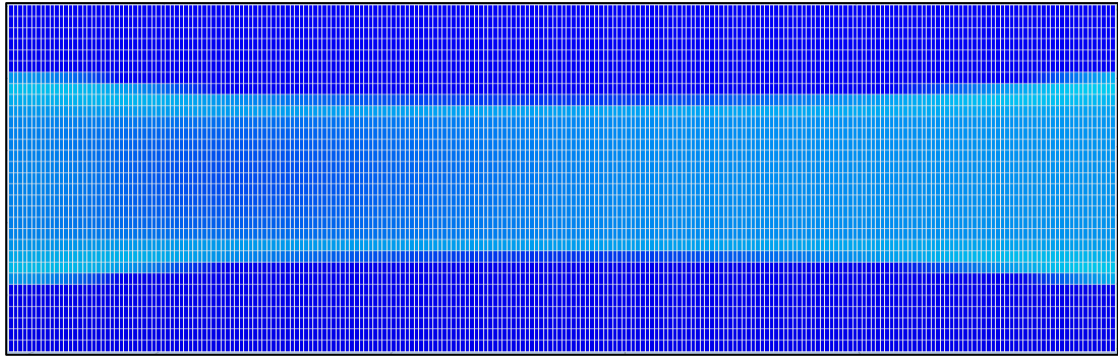
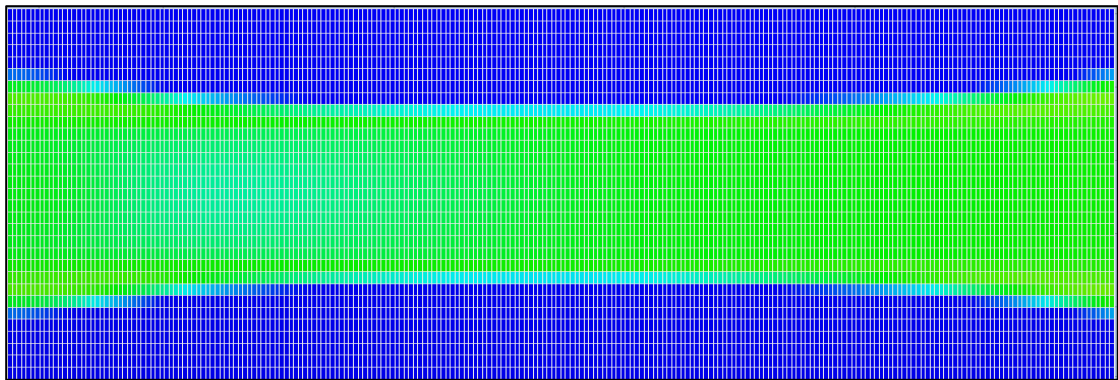


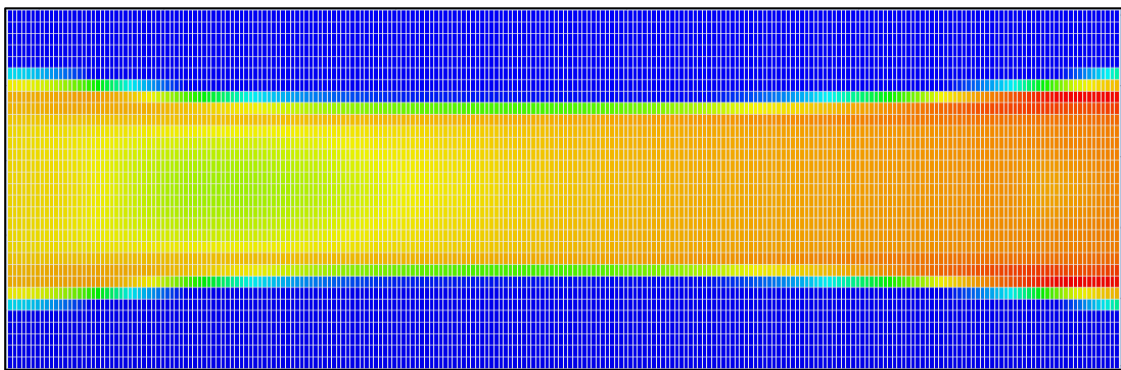
Figure 4.3 Gel components versus pore volume in production



1. At the beginning of the shut-in period



2. At the end of the shut-in period



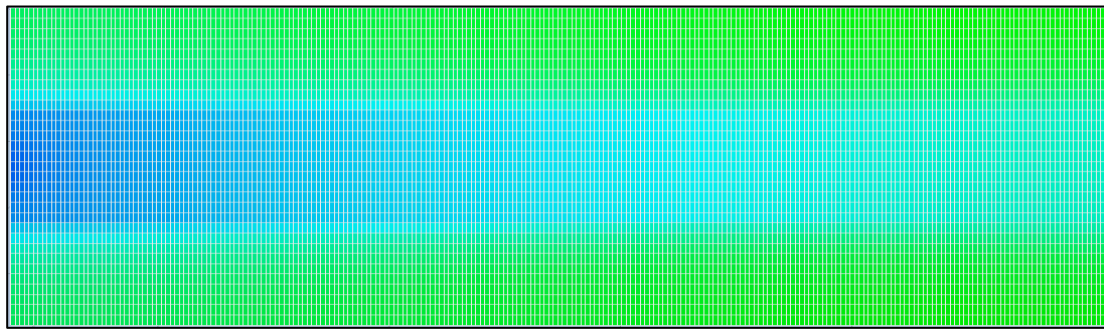
3. End of the production



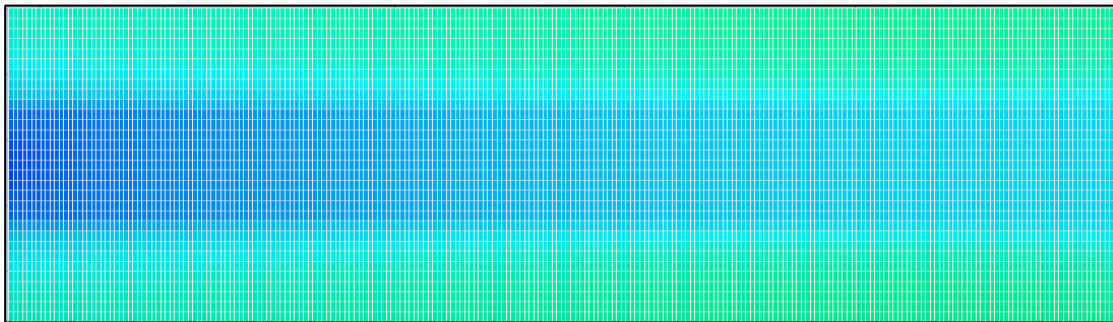
Figure 4.4 Cross-section from top: Gel in the core in different type steps

The first picture in Figure 4.4 shows that gel creation commences during the shut-in period in a high permeable zone. As the middle section turns green, it can be said that the amount of gel is escalating significantly, and the maximum level of gelation is observed in

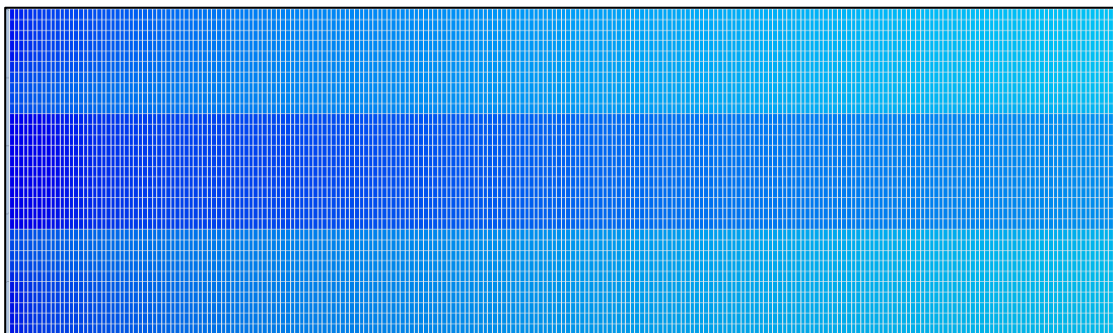
the third picture in Figure 4.4, which indicates the end of the production with an abundance of orange-red colours.



1. Pore volume: 0.48 (gel injection started)



2. Pore volume: 0.88 (shut-in period started)

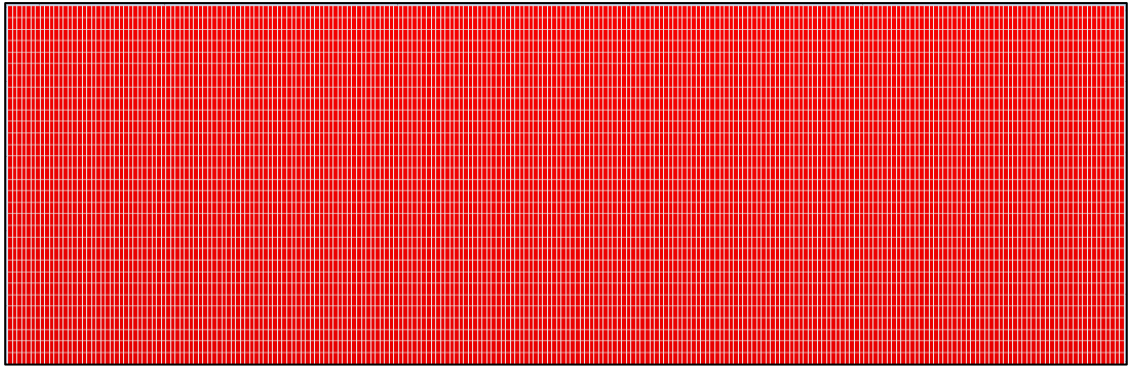


3. End of the production

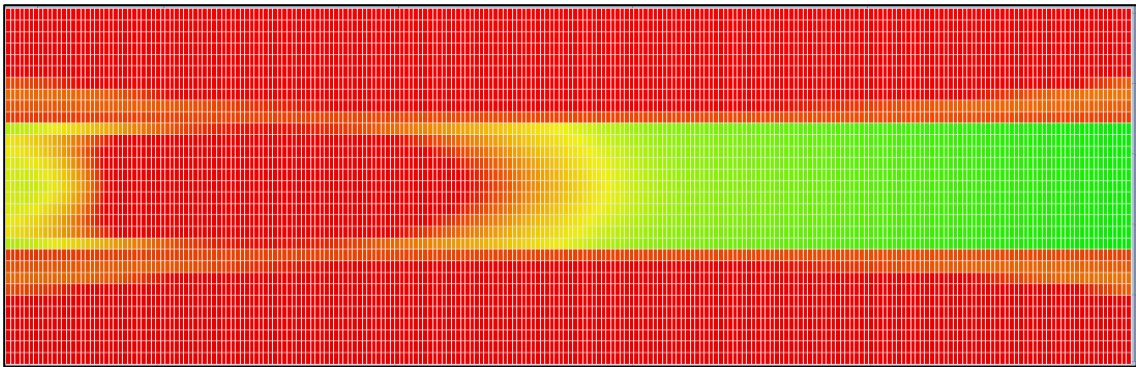


Figure 4.5 Cross-section from top: Oil saturation for Base case

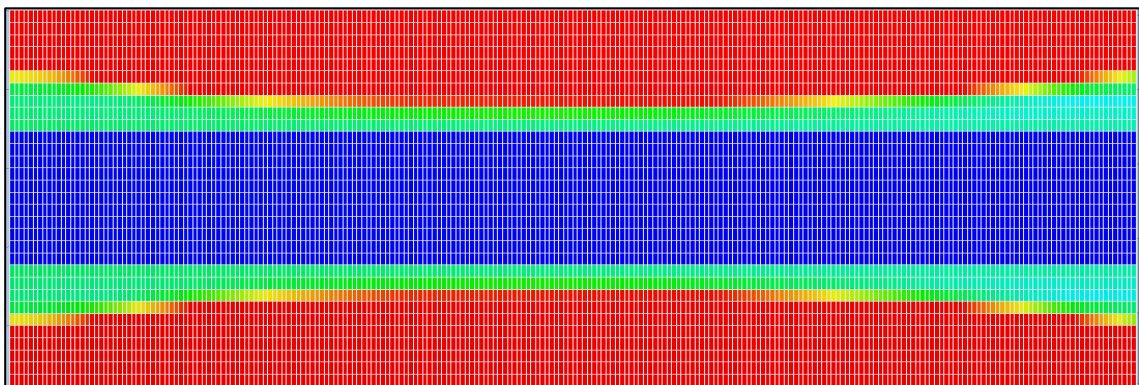
The oil saturation decreases gradually, shown in Figure 4.5, pore volume 0.48, 0.88, and minimum at the end of the production in the whole zone.



1. Pore volume: 0.48 (gel injection started)



2. After the shut-in period (shut-in period started)



3. End of the production



Figure 4.6 Cross-section from top: Water permeability reduction

Water was injected into the core in the first 6 hours, where the pore volume range was 0.0-0.48. The process was followed by 5 hours gel injection. At 0.88 pore volume well was shut-in, and 14 hours later, water permeability reduction was noticed, as shown in picture 2 in

Figure 4.6. Thus, at the end of the production, water permeability reduction was in its lowest number in the high permeable zone.

4.3.2 Case: Without gel

In this part, we assume that there are not gel components in injection fluid which simulation will give the production overview to compare with other experiments.

Water was used as the only component in injection fluid which we can observe the production rates differences Figure 4.7. All parameters of injection fluid such as injection rate, start & end time of injection are the same as base gel case. Instead of gel components, only water was injected into the core.

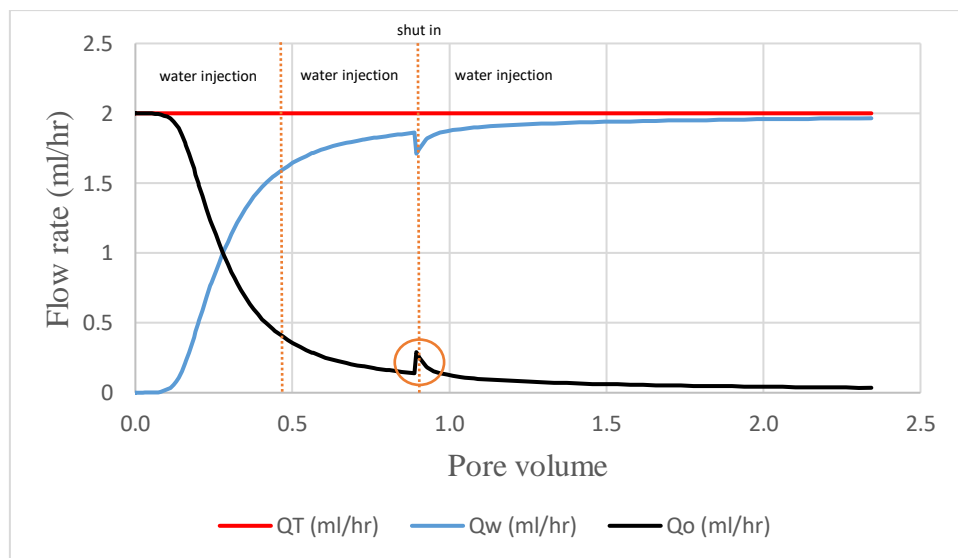
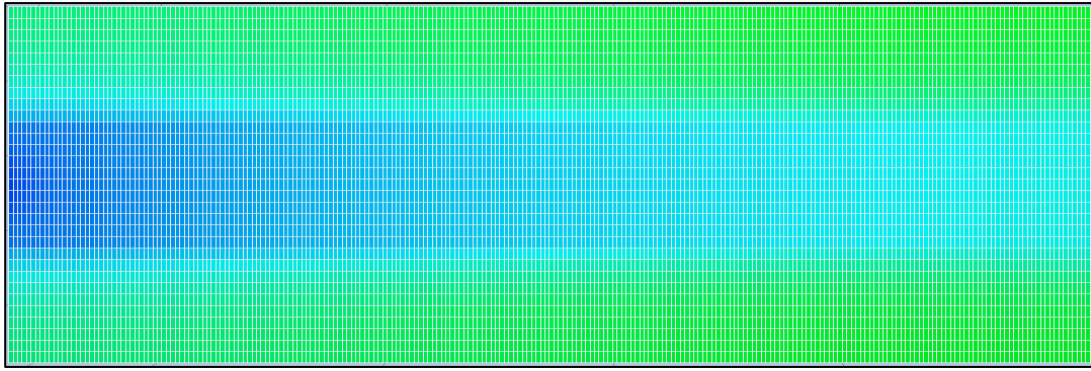
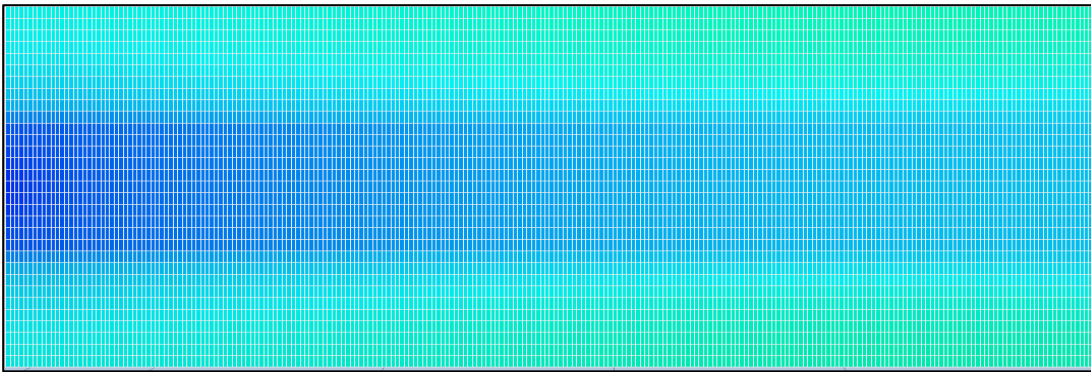


Figure 4.7 Production rates for Case: without gel

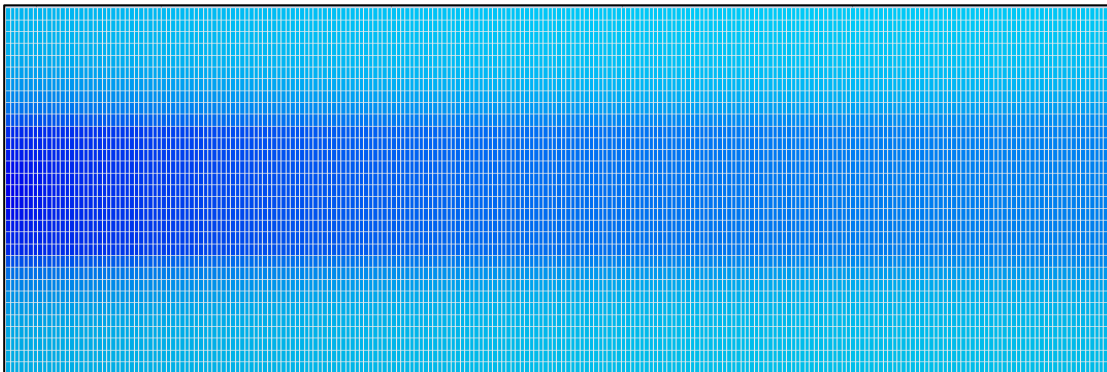
In the no gel case, the rising of oil production decreases dramatically compared with the Base case. It can be happened because of water traps around oil in no gel case.



1. Pore volume: 0.48 (at the beginning of the production)



2. Pore volume: 0.88 (shut-in period started)



3. End of the production



Figure 4.8 Cross-section from top: Oil saturation for Case: without gel

Decrement of oil saturation in the Case: without gel was detected from earlier phase till the end of the production in all over the core, Figure 4.8.

Comparison between Base case and without gel case is shown in Figure 4.9. For 0.48 pore volume, there was a slight difference in oil saturation between the Base case and Case: without gel, where oil saturation was lower in the Case: without gel. The same oil saturation reduction scenario was noticed at 0.88 pore volume. However, at the end of the production, it is obvious from the last pictures in Figure 4.9 the oil saturation in the Base case was moderately lower than the Case: without gel both in the high permeable and low permeable zone, which indicated the gelation effect.

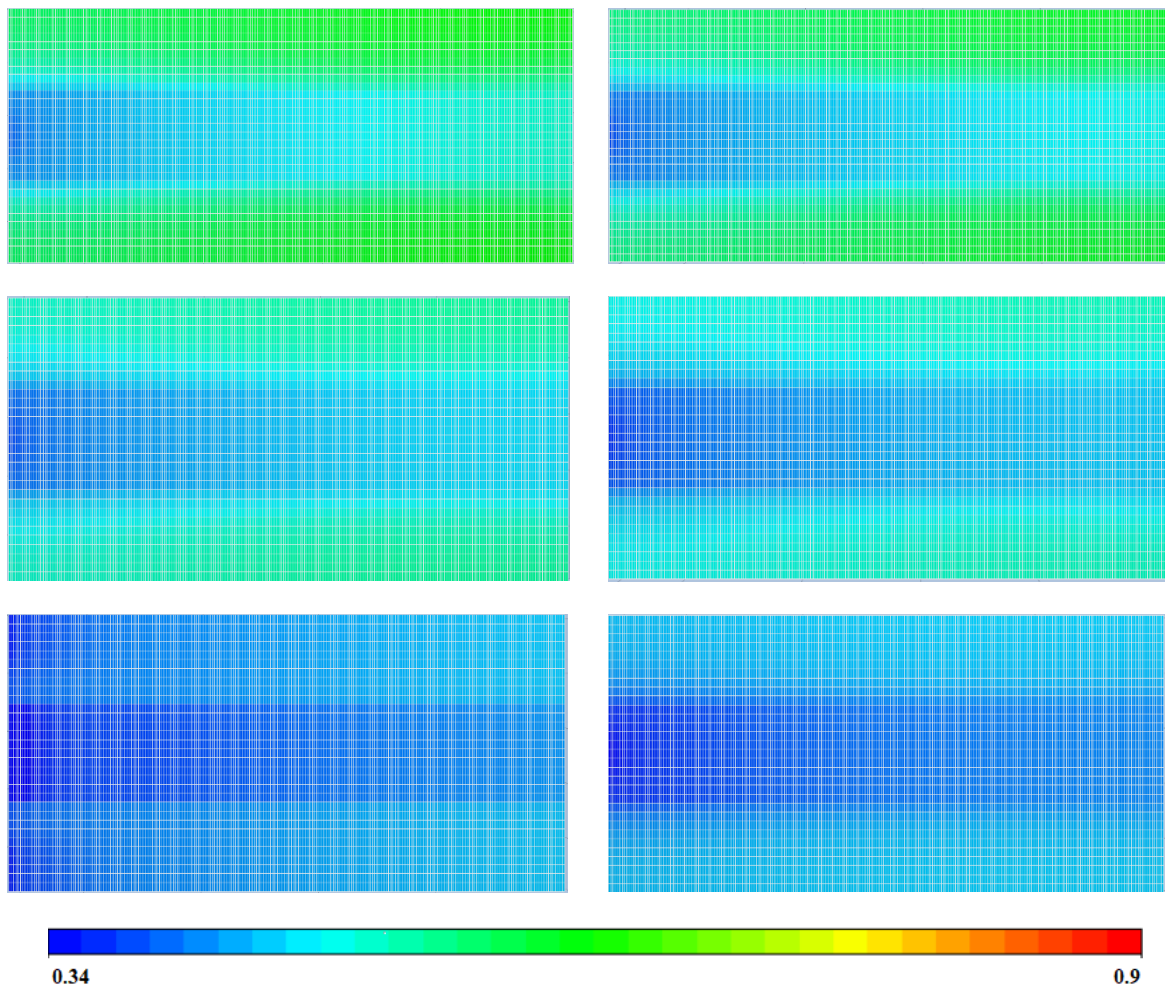


Figure 4.9 Cross-section from top: Oil saturation: Left side is Base case; Right side is Case: without gel

4.3.3 Effect of concentration

The concentration of gel components has obvious in the gelation process, according to the literature study. Therefore, three cases were implemented to see how the effect of the concentration of gel components on the gelation process by simulations.

4.3.3.1 Case 1 Laponite 1.5 % and HPAM 0.3%

In Case 1, we chose to inject fluid containing Laponite clay with 1.5 % and HPAM polymer 0.3% concentration at a 2 ml/h flow rate within 5 hours. First, gel components injection carried out at between 0.48 and 0.88 pore volume; then water injection started from 0.88 pore volume in Figure 4.10. Finally, the shut-in period was started to be processed in the 0.88 pore volume, 24 hours. As a result, we observed a straight increment in oil production for Case 1 comparing with a less straight (curved) increment for the Base case in Figure 4.10.

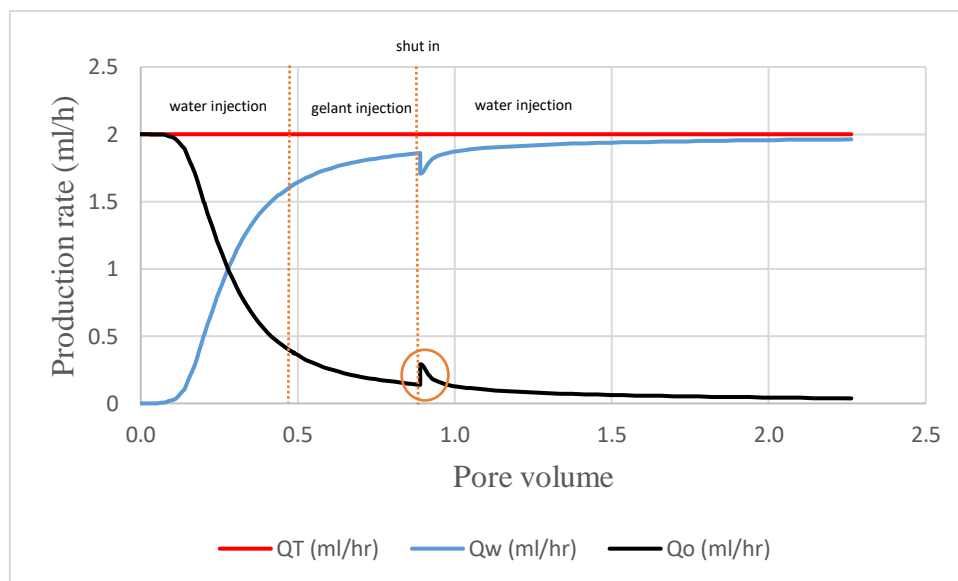


Figure 4.10 Production rates for Case 1

The amount of gel concentration in production is not comparable. Only a decrease in clay content is observed because of the low clay concentration of injected fluid compared with Base case Figure 4.11.

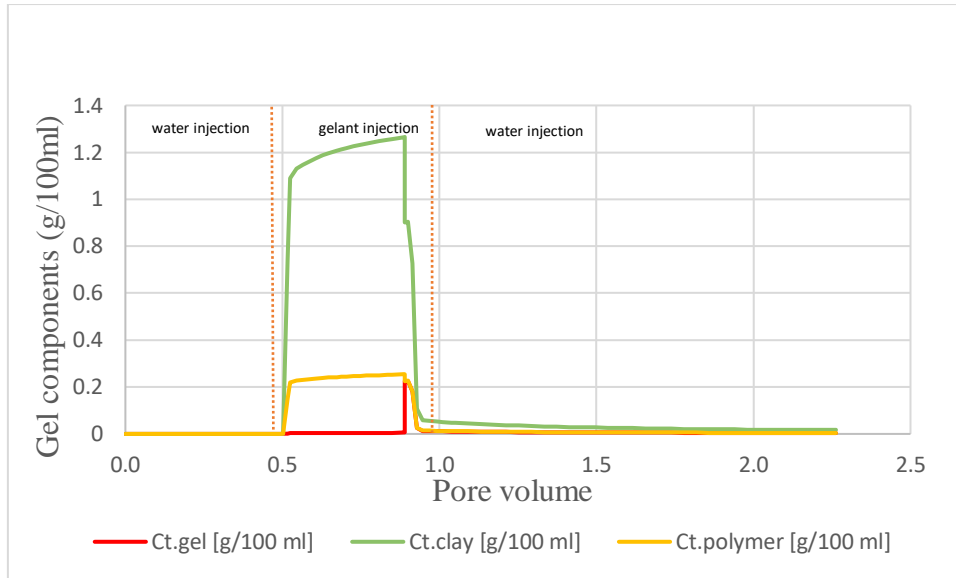


Figure 4.11 Gel components versus pore volume in production

4.3.3.2 Case 2 Laponite 1.0 % and HPAM 0.3%

In Case 2, we chose to inject fluid containing Laponite clay with 1.0 % and HPAM polymer 0.3% concentration at a 2 ml/h flow rate within 5 hours. Gel components injection carried out at between 0.48 and 0.88 pore volume; then water injection started from 0.88 pore volume Figure 4.12. The shut-in period was started to be processed in the 0.88 pore volume, 24 hours. We observed straight increment then sharp decrement in oil production for Case 2 in Figure 4.12. The influence of clay on the gelation process is easily observed, which low clay content cause a little increment in oil production. The result of Case 2 can be considered as a resemblance of Case: without gel.

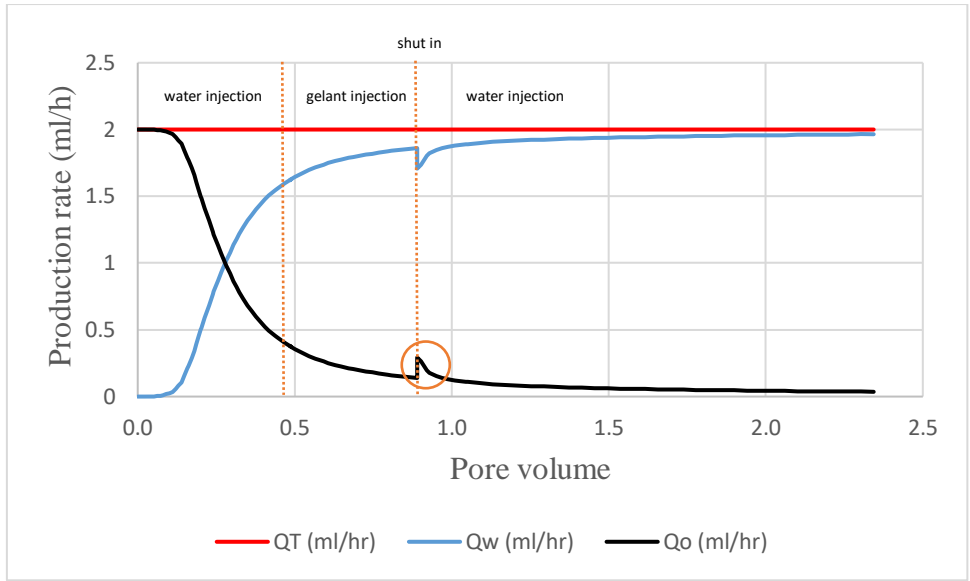


Figure 4.12 Production rate for Case 2

The amount of gel concentration in production is not comparable. Only a decrease in clay content is observed because of the low clay concentration of injected fluid compared with base case and Case 1, Figure 4.13.

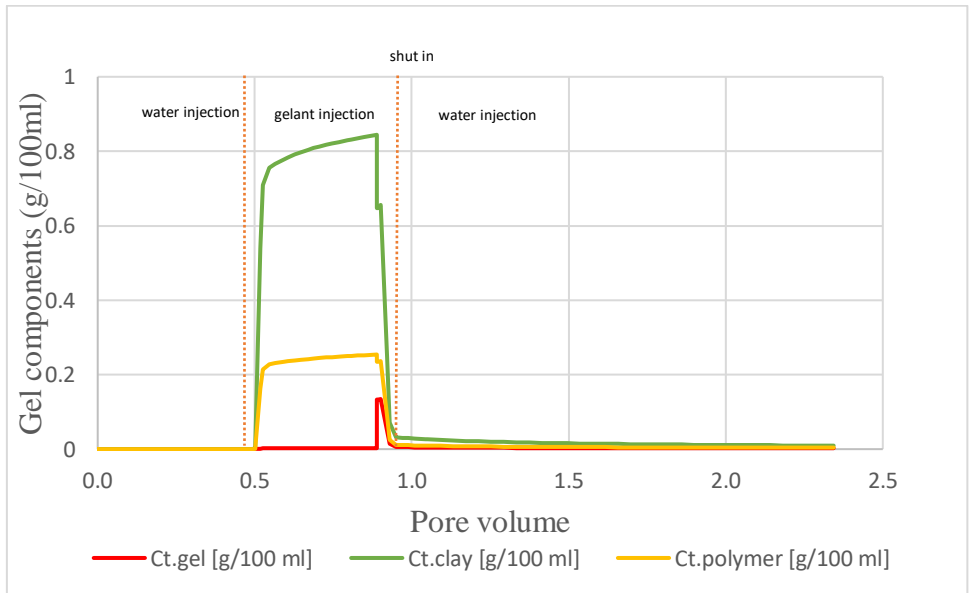


Figure 4.13 Gel components versus pore volume in production

4.3.3.3 Case 3 Laponite 1.0 % and HPAM 0.03%

In Case 3, we chose to inject fluid containing Laponite clay with 1.0 % and HPAM polymer 0.03% concentration at a 2 ml/h flow rate within 5 hours. Gel components injection carried out at between 0.48 and 0.88 pore volume; then water injection started again from 0.88 pore volume in Figure 4.14. The shut-in period was started to be processed in the 0.88 pore volume, 24 hours. We observed a straight increment in oil production for Case 3 in Figure 4.14. The effect of clay in the gelation process in Case 3 is not observable, which the same tendency in oil production of the Base case can be seen in Case 3.

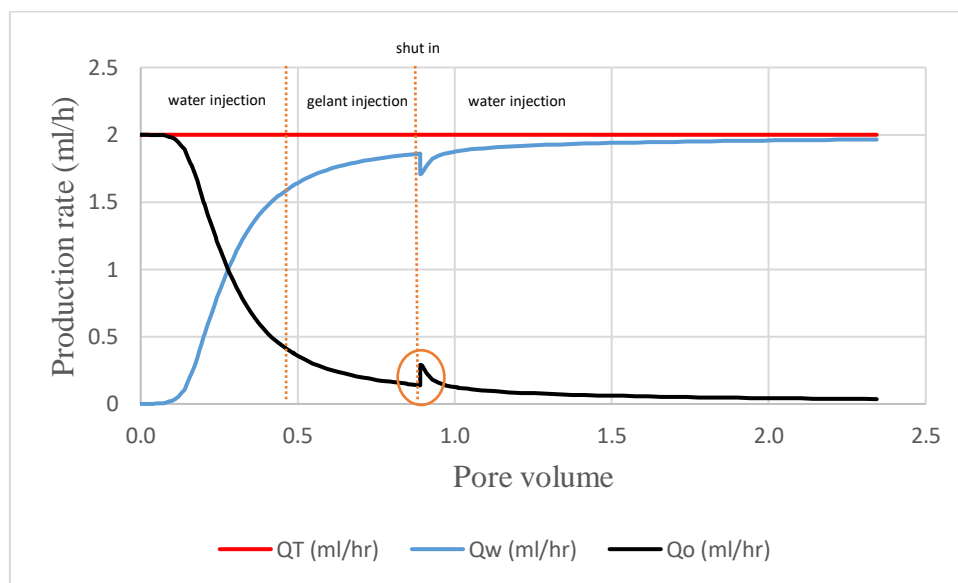


Figure 4.14 Production rates for Case 3

The amount of gel concentration in production is not comparable. Only an increase in clay content is observed because of the low clay concentration of injected fluid compared with the Base case (Figure 4.15).

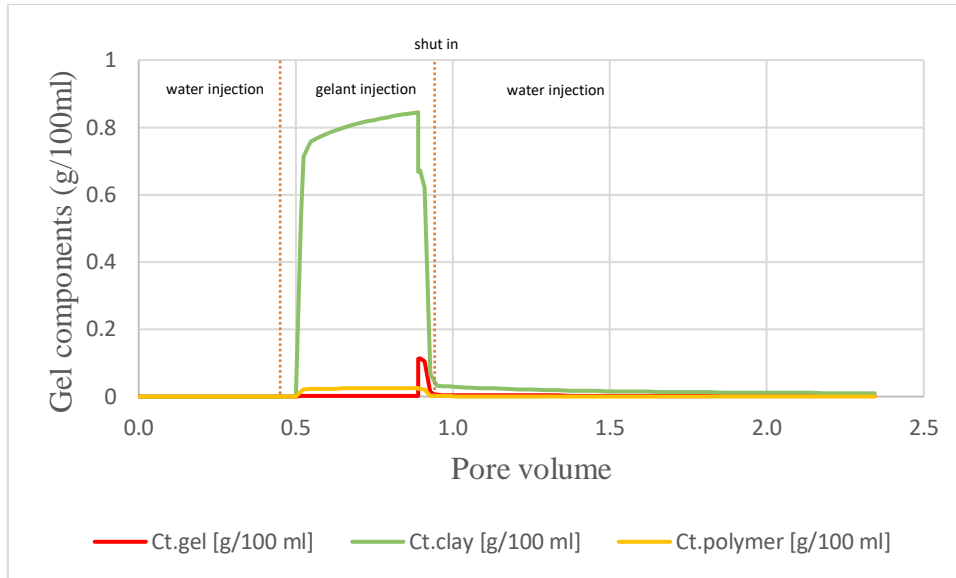


Figure 4.15 Gel components versus pore volume in production

Summing up the result above, the gel was formed in Case 1, Laponite clay 1.0% and HPAM 0.03%. Therefore, decreasing the proportion of gel components can cause a negative effect on the forming of gel.

4.3.4 Effect of shut-in period

In this part, two simulations with 5 hours and 36 hours shut-in period were carried out to see the impact of the shut-in period on the gel-forming.

4.3.4.1 Case 4 Shut-in 5 hours

In Case 4, we chose to inject fluid containing Laponite clay with 2 % and HPAM polymer 0.3% concentration at a 2 ml/h flow rate within 5 hours. As a result, gel components injection carried out at between 0.48 and 0.88 pore volume; then water injection started again from 0.88 pore volume in Figure 4.16. Therefore, the shut-in period was started to be processed in the 0.88 pore volume, 5 hours.

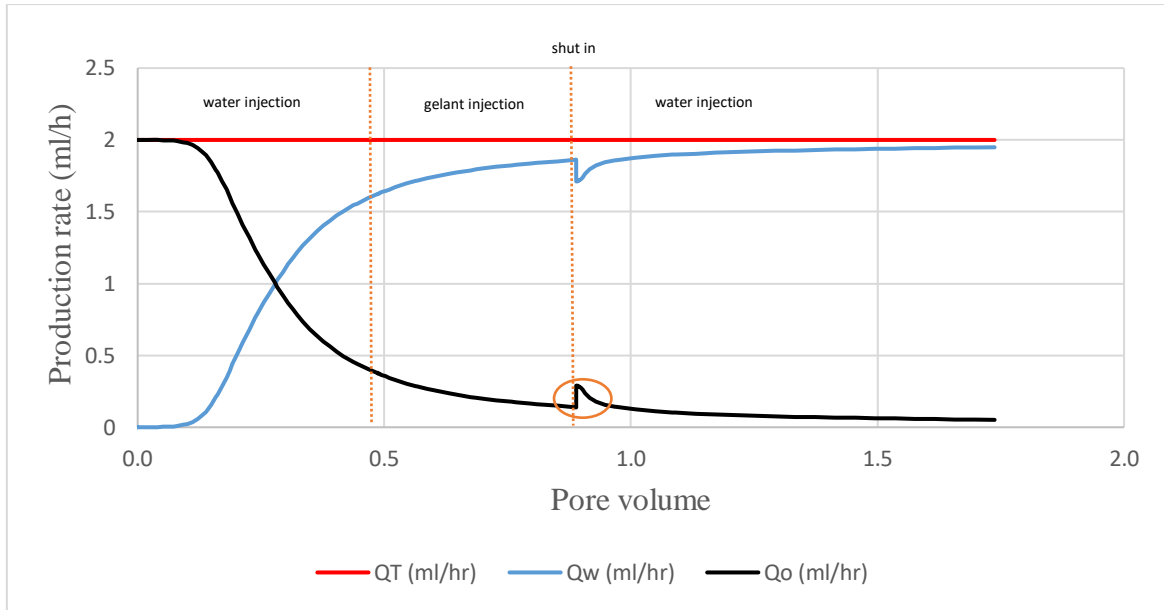


Figure 4.16 Production rates for Case 4

From Figure 4.16, the effect of gelation can be observed at around 0.88 pore volume with raising in oil and decreasing in water production, respectively. Therefore, the injection time of gel components is not enough to create appropriate gel flooding in the reservoir due to a lower shut-in period than gelation time.

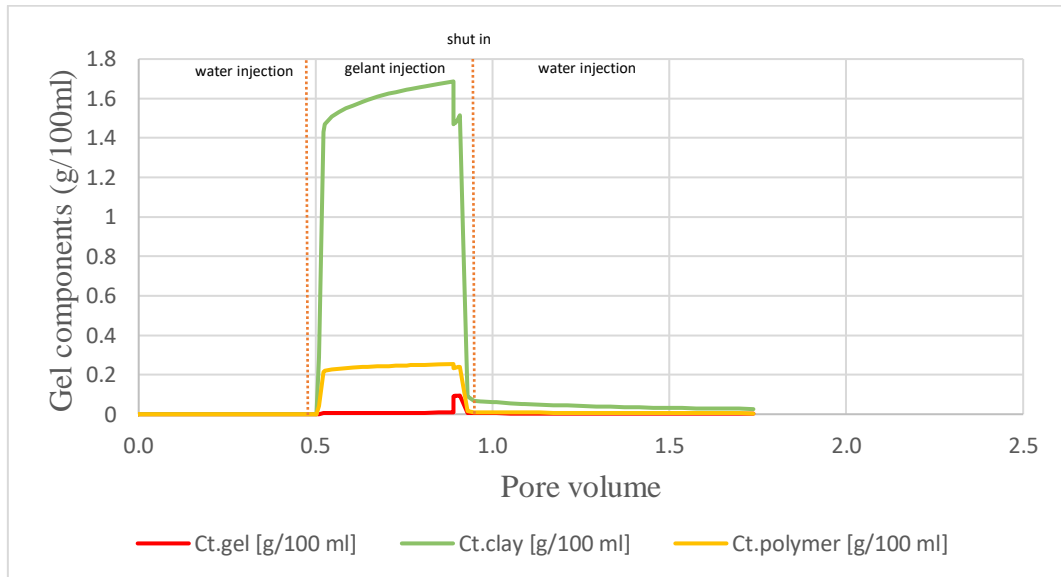


Figure 4.17 Gel components versus pore volume in production

The proportion of gel components in production is observed as in Figure 4.17. Production of gel components almost at the same initiation time of injection. We observed gel in

production flow after 0.89 pore volume because of 5 hours shut-in period. Gel production decreases dramatically after 0.9 pore volume, and we observe a stop in gel production at 1.4 pore volume. It can be seen that the shut-in period should not be less than gelation time.

4.3.4.2 Case 5 Shut-in 36 hours

In Case 5, we chose to inject fluid containing Laponite clay with 2 % and HPAM polymer 0.3% concentration at a 2 ml/h flow rate within 5 hours. As a result, gel components injection carried out at between 0.48 and 0.88 pore volume; then water injection started again from 0.88 pore volume, Figure 4.18. Therefore, the shut-in period was started to be processed in the 0.88 pore volume, 36 hours.

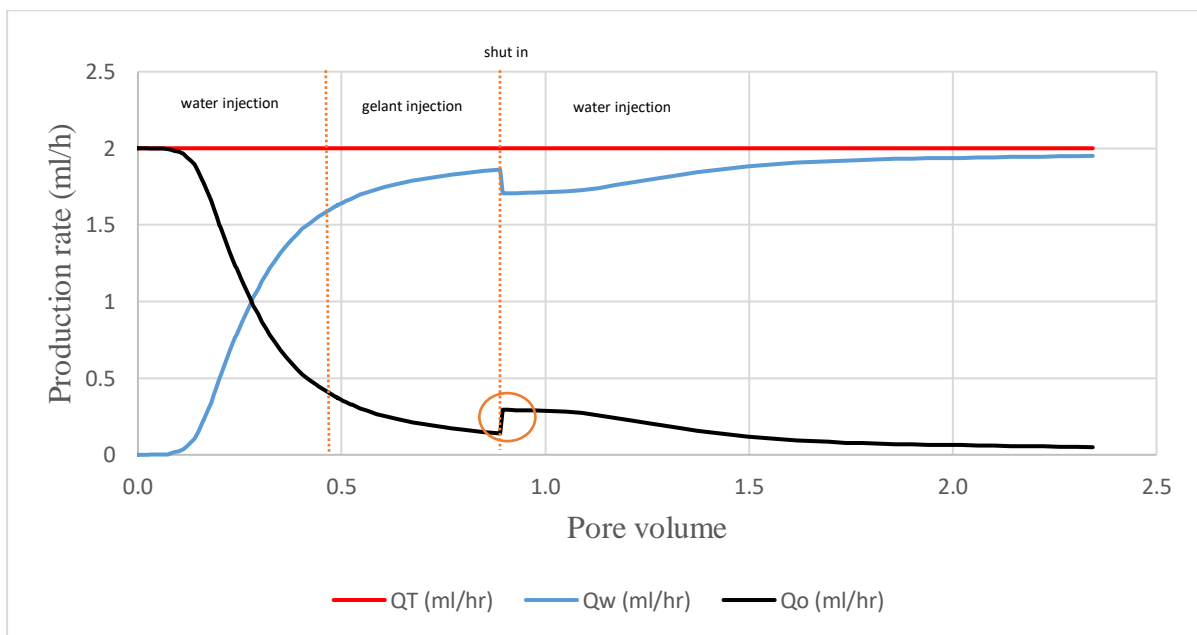


Figure 4.18 Production rates for Case 5

From Figure 4.18, gelation can be observed at around 0.9 pore volume with raising in oil and decreasing water production. We could not see any differences in production rate for the sake of the shut-in period. The results from Case 5 and Case 4 are the same as the Base case. Thus the effect of the shut-in period on oil gelation cannot be observed clearly by this simulation program.

The proportion of gel components in production is observed as in Figure 4.19. Production of gel components started almost at the same initiation time of injection with a slight delay, but this time is enough to have the gelation process in the core. Gel production decreases slightly, and it stops at the end of the production.

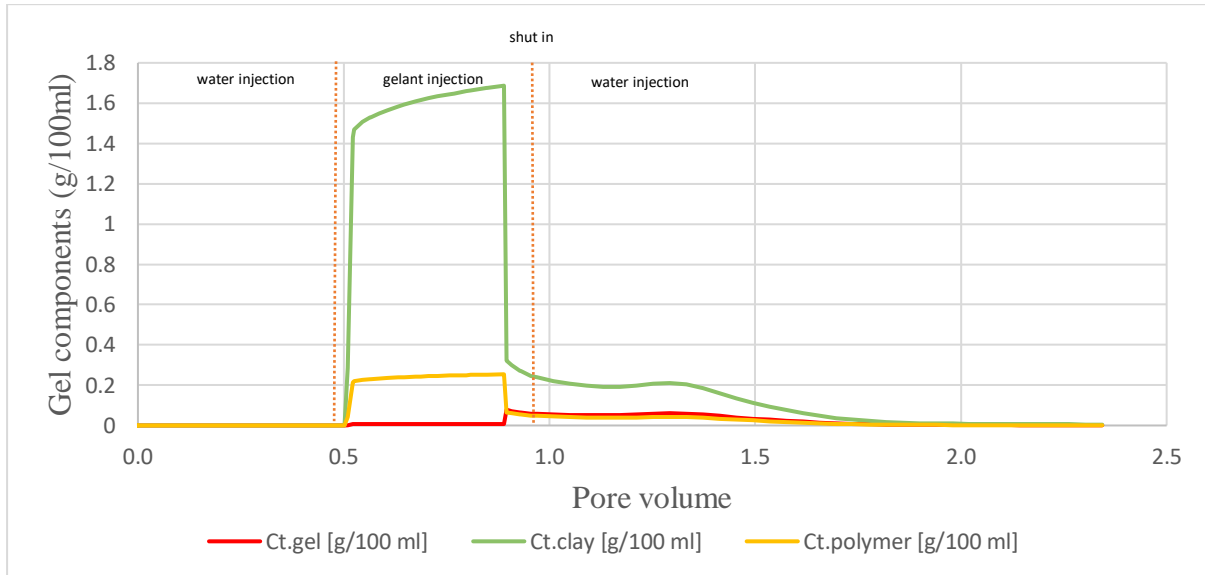


Figure 4.19 Gel components versus pore volume in production

Taking gelation time into account, 5 hours shut-in time, which was smaller than gelation time, was not enough for gel-forming. Otherwise, we saw a positive effect on oil production as the shut-in period rose, such as Case 5.

4.3.5 Recovery factor affected by gel treatment for each case

Seven different oil recovery factors are obtained by simulation. However, simulating the Base case can be considered the best option as for oil recovery factor, 48% for 2.3 pore volume, Figure 4.21. Changing only the shut-in period can result in oil recovery: The increasing shut-in period from 24 hours to 36 hours will not change the oil recovery trend; thus, oil recovery follows the same line in the Base case and Case 5. Shut-in periods for the Base case and Case 5 are higher than the calculated gelation time. The gelation period is not enough with 5 hours shut in the period, so gelation is not observed for Case 4. Gelation time for Case 1 is 23.7 hours

which is not enough time to observe the effect of gel with 24 hours shut-in period. The same tendency is shown for Case 2 and Case 3, where the shut-in period is considerably lower than gelation time. Oil recovery line for Case: without gel overlaps Case 1, Case 2, and Case 3, Figure 4.21.

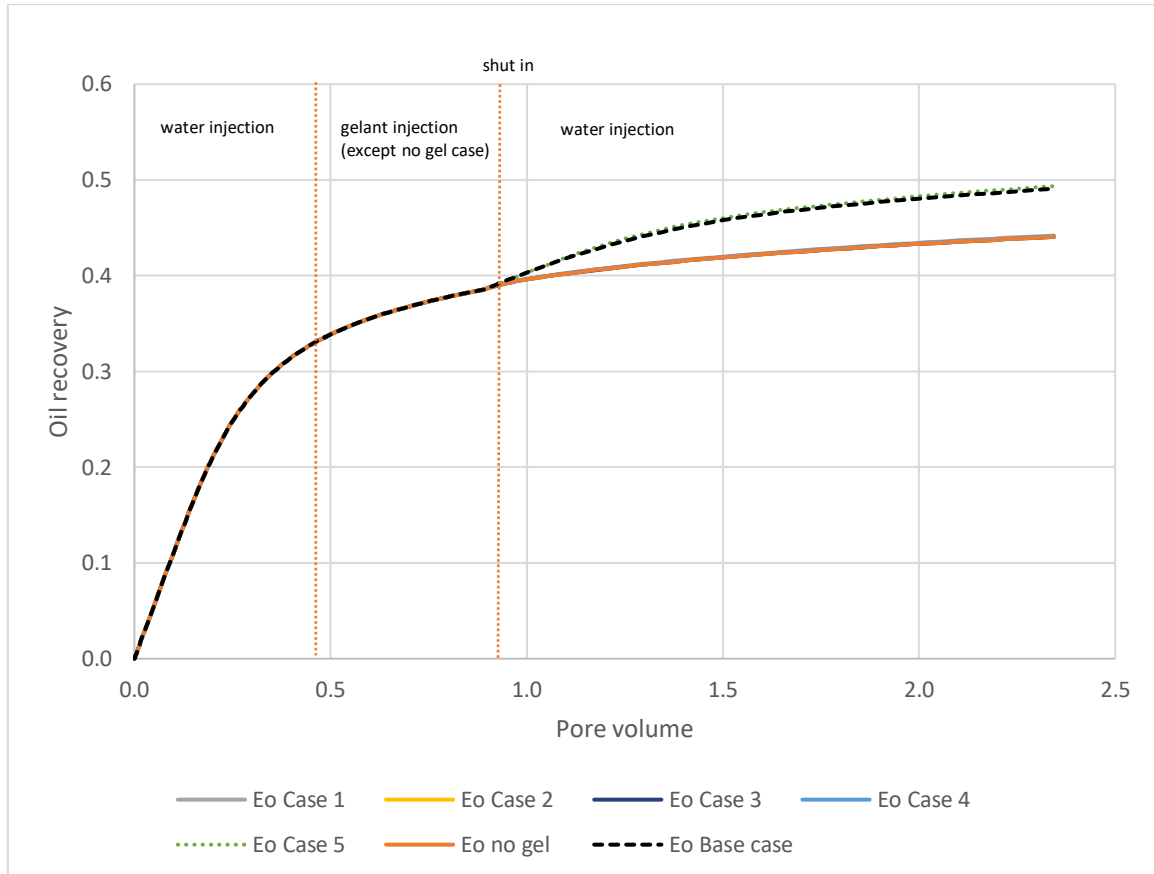


Figure 4.20 Recovery factors for all cases in different pore volume Base case (clay 2% and polymer 0.3%) Case 1 (clay 1.5% and polymer 0.3) Case 2 (clay 1% and polymer 0.3) Case 3 (clay 1% and polymer 0.03) Case 4 decreased shut in time to 5hours Case 5 increased shut in time to 36hours

Figure 4.21 shows that the relation between pressure drop and gelation process is proportional. Higher pressure drop can be seen with gelation, Case 5. The pressure drop for the Base case is slightly lower than Case 5 because the shut-in period for Case 5 is more than the Base case. It is also possible to see the effect of the gelation period of Case 1, 23.7 hours gelation time. The gelation time of Case 1 is almost the same as the shut-in period, so that gelation can be observed here. Case: without gel, Case 2, Case 3 and Case 4 shows the same scenario for pressure drop.

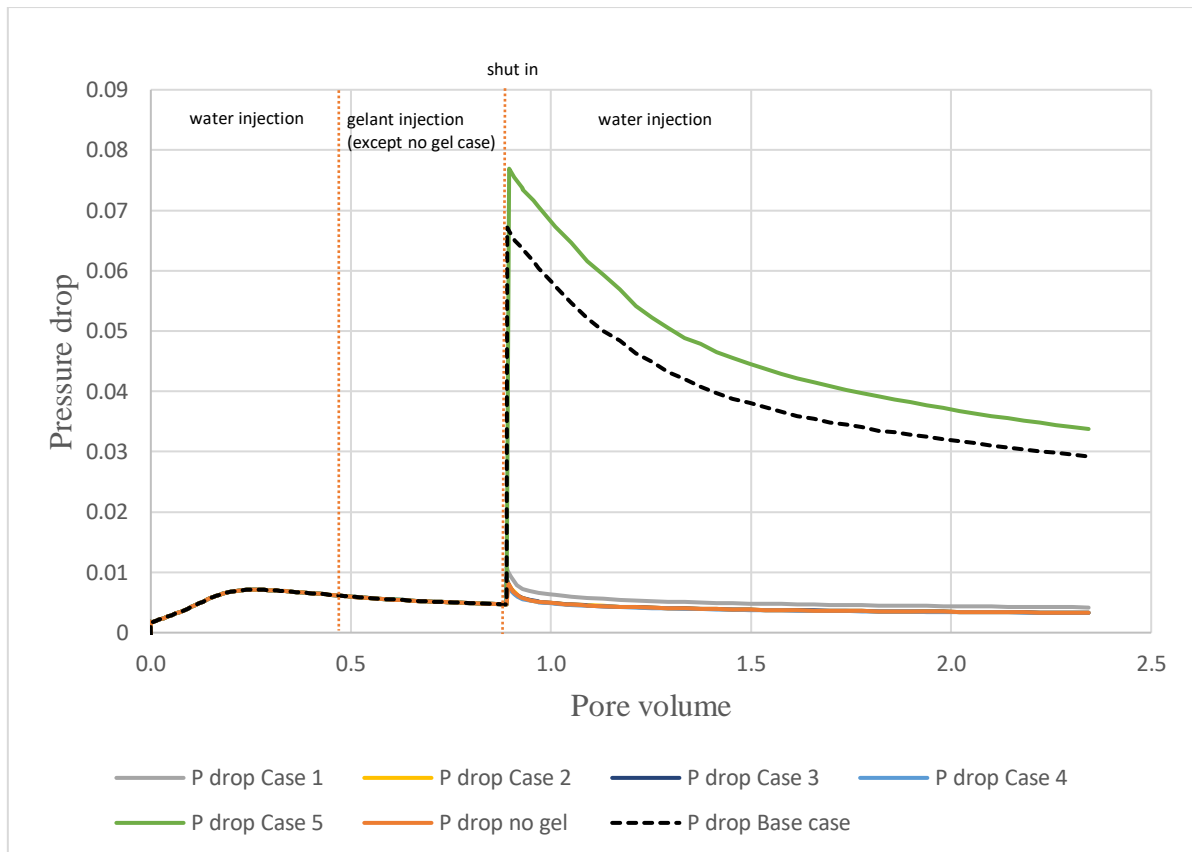


Figure 4.21 Pressure drop for all cases Base case (clay 2% and polymer 0.3%) Case 1 (clay 1.5% and polymer 0.3) Case 2 (clay 1% and polymer 0.3) Case 3 (clay 1% and polymer 0.03) Case 4 decreased shut in time to 5hours Case 5 increased shut in time to 36hours

4.4 Gel in the core

Figure 4.22 demonstrates various gel forming in the core for 7 cases. The amount of gel for Case 5 is higher than all the cases, which shows that 36 hours shut-in period is an appropriate time for seeing the effect of gelation in Figure 4.22 (d). Comparing Base case and Case 1, the amount of gel for the Base case is more than Case 1 due to the concentration change in clay component in Figure 4.22 (a), (b).

As for the other cases in Figure 4.22 (c), the amount of gel is not noticed in the core because of how much gel component injected the same amount are produced. It means the shut-in period is not enough to see gelation in the core.

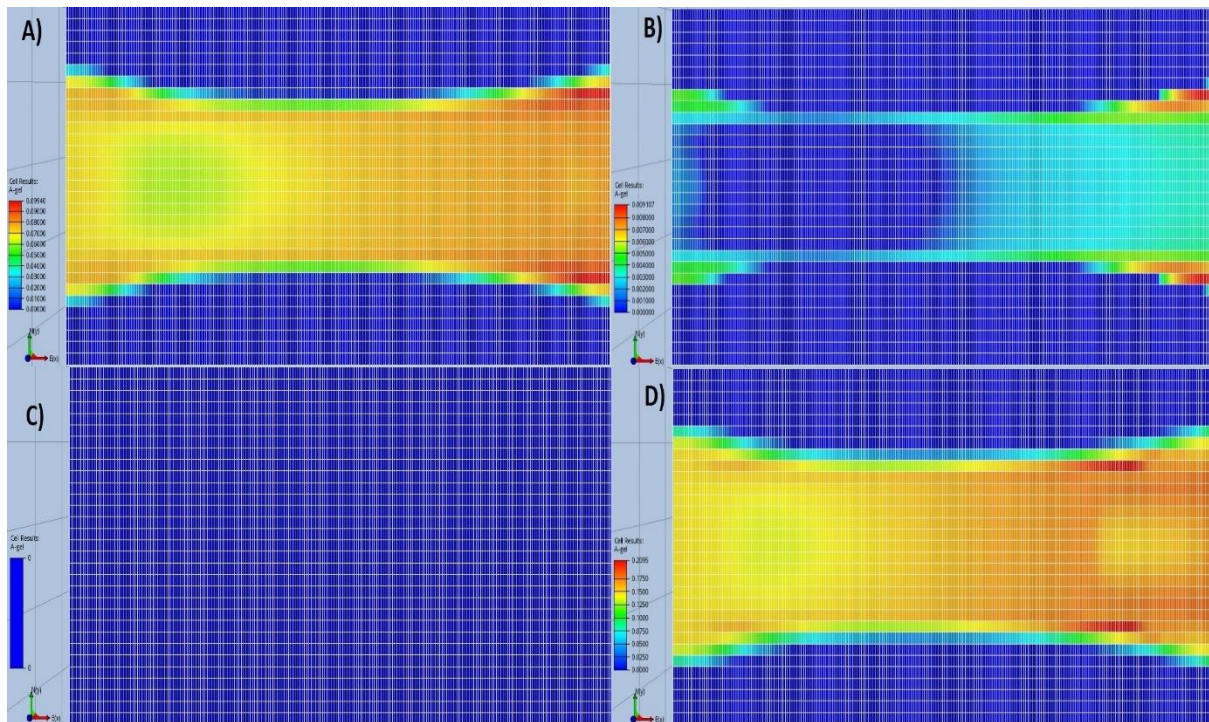


Figure 4.22 Cross-section from top: A- Base Case B- Case 1 C- Case: No gel D- Case 5 at the end of the production

4.5 Discussion

According to the literature (Adijat, 2019), Laponite-PEG, Laponite-Gellan gum, and Laponite-HPAM interactions were analysed. Laponite-HPAM interaction was selected as the strongest gel components to form a gel. Results from the simulation were appropriate to the literature; it represented the effectiveness of Laponite-HPAM interaction and proportional relation between gel strength and concentration of Laponite clay. Because of the applicability of simulation and the limited period, it was not possible to simulate various polymers such as PEG and Gellan gum. In the laboratory condition, a gel retarder was used in some cases where its effects could be observed on gel treatment, but a retarder was not considered in the simulation.

The results reported in this thesis are not without limitations. In this thesis, reservoir conditions are relevant for well that have been cooldown due to long time sea water injection because gelant injections were carried out at room temperature. In contrast, gel activation was carried out in the oven at 50°C, representing further into the reservoir. The simulation doesn't show the proper effect of gelation as small changes in clay concentration.

4.6 Further work

The work done in this thesis has examined gels prepared with Laponite clay and HPAM polymer. However, in-depth studies should be done to qualify the system properly. The following recommendations for future work can improve our knowledge and effectively the quality of gels.

- Further experiment and simulation should be done to examine the effect of Laponite-HPAM interactions with different concentrations.
- It should also be investigated how the ionic composition of the brine will affect Laponite-HPAM gel formation.
- Further tests should be conducted to verify the stability of these gels over more extended periods at various temperatures and their resistance to syneresis to establish their potential for use in reservoirs with higher temperatures.
- Nanocomposite gels could be evaluated in core plugs with various fracture patterns and sizes to determine their application range.
- Other polymers, such as PEG and Gellan gum, may have potential use together with Laponite. Relevant input values for these polymers should be generated in experiments before gelation experiments can be modelled and the potential for using Laponite together with these polymers can be determined.

Chapter 5 Conclusions

This thesis investigated the gelation effect in core plug by IORCoreSim simulation software. Several cases were simulated, and results from those simulations were described. Furthermore, the theoretical background of the gelation process, existing experimental researchers, were indicated in detail as the gel component clay and polymer were used with different concentration for each case.

Following are conclusions that can be obtained out of this study:

1. Three experiments were carried out in the laboratory. Gel code 4 (Deformable upper part with high flow resistance) was observed in the systems of 2% Laponite and 0.3% HPAM, and 1.0% Laponite with 0.3% HPAM. Gel code 3 (Highly viscous and deformable flowing fluid) was observed in the system of 1.0% Laponite with 0.03% HPAM. It was concluded that the system with 2.0% Laponite and 0.3% HPAM interaction was the most promising option to form a gel. The gelation time is too long for low Laponite clay and low HPAM concentrations.
2. Parameters for the calculation of gel time for Laponite/HPAM systems can be tuned against the experimental results and then used as input in the simulations.
3. IORCoreSim can be used for simulation of placement of Laponite/HPAM gels in fractured core plug experiments.
4. The simulator has been used to study gel placement in fractured core plug using various concentration and shut-in times.
5. Simulations are clearly showing that the shut-in time should be longer than the gelation time .
6. IORCoresim simulation is appropriate to observe the effects of Laponite/HPAM interactions with different gel component concentrations and conditions for the sake of gel-forming.

References

1. Ahmadi, M.A., Chen, Z., 2019. Comparison of machine learning methods for estimating permeability and porosity of oil reservoirs via petro-physical logs. *Petroleum* 5, 271–284. <https://doi.org/10.1016/j.petlm.2018.06.002>
2. Ahmed, T.H., 2001. *Reservoir engineering handbook*, 2nd Gulf Professional Pub, Boston.
3. Al-Anazi, H.A., Sharma, M.M., 2002, January. Use of a pH-sensitive polymer for conformance control. In *International Symposium and Exhibition on Formation Damage Control*. Society of Petroleum Engineers.
4. Al-Hajri, S., Mahmood, S., Abdulelah, H., Akbari, S., 2018. An Overview of Polymer Retention in Porous Media. *Energies* 11, 2751. <https://doi.org/10.3390/en11102751>
5. Ardebili, H., Zhang, J., Pecht, M.G., 2019. 6 - Characterization of encapsulant properties, in Ardebili, H., Zhang, J., Pecht, M.G. (Eds.), *Encapsulation Technologies for Electronic Applications (Second Edition)*, Materials and Processes for Electronic Applications. William Andrew Publishing, pp. 221–258. <https://doi.org/10.1016/B978-0-12-811978-5.00006-7>
6. Arekhov, V., Hincapie, R.E., Clemens, T., 2020. Wettability Changes and Interfacial Tension Reduction in Alkali Polymer Flooding of High and Low Tan Number Oils. Presented at the SPE Europec, OnePetro. <https://doi.org/10.2118/200591-MS>
7. Banerjee, S., Tyagi, A.K., 2011. *Functional Materials: Preparation, Processing and Applications*. Elsevier, St. Louis, UNITED STATES.
8. Chauveteau, G., 1981. Molecular Interpretation of Several Different Properties of Flow of Coiled Polymer Solutions Through Porous Media in Oil Recovery Conditions. Presented at the SPE Annual Technical Conference and Exhibition, OnePetro. <https://doi.org/10.2118/10060-MS>
9. Chauveteau, G., Tabary, R., Le Bon, C., Renard, M., Feng, Y., Omari, A., 2003. In-Depth Permeability Control by Adsorption of Soft Size-Controlled Microgels. Presented at the SPE European Formation Damage Conference, OnePetro. <https://doi.org/10.2118/82228-MS>
10. Coste, J.-P., Liu, Y., Bai, B., Li, Y., Shen, P., Wang, Z., Zhu, G., 2000. In-Depth Fluid Diversion by Pre-Gelled Particles. Laboratory Study and Pilot Testing. Presented at the SPE/DOE Improved Oil Recovery Symposium, OnePetro. <https://doi.org/10.2118/59362-MS>
11. Cummins, H.Z., 2007. Liquid, glass, gel: The phases of colloidal Laponite. *Journal of Non-Crystalline Solids*, 353(41-43), pp.3891-3905.
12. Delshad, M., Kim, D.H., Magbagbeola, O.A., Huh, C., Pope, G.A., Tarahhom, F., 2008. Mechanistic Interpretation and Utilization of Viscoelastic Behavior of Polymer Solutions for Improved Polymer-Flood Efficiency. Presented at the SPE Symposium on Improved Oil Recovery, OnePetro. <https://doi.org/10.2118/113620-MS>

13. Druetta, P., Raffa, P., Picchioni, F., 2019. Chemical enhanced oil recovery and the role of chemical product design. *Applied Energy* 252, 113480. <https://doi.org/10.1016/j.apenergy.2019.113480>
14. El-Diasty, A.I., Aly, A.M., 2015. Understanding the Mechanism of Nanoparticles Applications in Enhanced Oil Recovery. Presented at the SPE North Africa Technical Conference and Exhibition, OnePetro. <https://doi.org/10.2118/175806-MS>
15. Fielding, R.C., Gibbons, D.H., Legrand, F.P., 1994. In-Depth Drive Fluid Diversion Using an Evolution of Colloidal Dispersion Gels and New Bulk Gels: An Operational Case History of North Rainbow Ranch Unit. Presented at the SPE/DOE Improved Oil Recovery Symposium, OnePetro. <https://doi.org/10.2118/27773-MS>
16. Fletcher, A.J., Davis, J.P., 2010. How EOR Can be Transformed by Nanotechnology. Presented at the SPE Improved Oil Recovery Symposium, OnePetro. <https://doi.org/10.2118/129531-MS>
17. Green, 2018. Enhanced Oil Recovery, Second Edition <http://store.spe.org/Enhanced-Oil-Recovery-Second-Edition-P1076.aspx> .
18. Green, D.W., Willhite, G.P., 1998. Enhanced oil recovery. Henry L. Doherty Memorial Fund of AIME, Society of Petroleum Engineers, Richardson, TX.
19. Guo, H., Li, Y., Wang, F., Yu, Z., Chen, Z., Wang, Y., Gao, X., 2017. ASP Flooding: Theory and Practice Progress in China. *Journal of Chemistry* 2017, e8509563. <https://doi.org/10.1155/2017/8509563>
20. Han, D., Yang, P., Luo, Y., Qingxia, W., Qingxia, L., Cheng, S., Shong, Z., Tang, J., Tang, X., 1998. Flow Mechanism Investigation and Field Practice for Low Concentration Flowing Gel. Presented at the SPE International Oil and Gas Conference and Exhibition in China, OnePetro. <https://doi.org/10.2118/50929-MS>
21. Imqam, A.H., 2015. Particle gel propagation and blocking behaviour through high permeability streaks and fractures. Missouri University of Science and Technology.
22. Imqam, A., Wang, Z., Bai, B., 2017. The plugging performance of preformed particle gel to water flow through large opening void space conduits. *Journal of Petroleum Science and Engineering* 156, 51–61. <https://doi.org/10.1016/j.petrol.2017.04.020>
23. Jennings, R.R., Rogers, J.H., West, T.J., 1971. Factors Influencing Mobility Control By Polymer Solutions. *Journal of Petroleum Technology* 23, 391–401. <https://doi.org/10.2118/2867-PA>
24. Jerauld, G., Webb, K., Lin, C.-Y., Seccombe, J., 2008. Modelling Low-Salinity Waterflooding. *SPE Reservoir Evaluation & Engineering - SPE RESERV EVAL ENG* 11, 1000–1012. <https://doi.org/10.2118/102239-PA>
25. Joshi, Y.M., 2007. Model for cage formation in a colloidal suspension of laponite. *The Journal of Chemical Physics* 127, 081102. <https://doi.org/10.1063/1.2779026>
26. J.Sheng, J., 2013. Enhanced Oil Recovery Field Case Studies. Gulf Professional Publishing.
27. Kamal, M.S., Adewunmi, A.A., Sultan, A.S., Al-Hamad, M.F., Mehmood, U., 2017. Recent Advances in Nanoparticles Enhanced Oil Recovery: Rheology, Interfacial Tension, Oil Recovery, and Wettability Alteration. *Journal of Nanomaterials* 2017, e2473175. <https://doi.org/10.1155/2017/2473175>

28. Kantzas, A., Marentette, D.F., Allsopp, K., 1999. Utilization of Polymer Gels, Polymer Enhanced Foams, And Foamed Gels For Improving Reservoir Conformance. *Journal of Canadian Petroleum Technology* 38. <https://doi.org/10.2118/99-13-58>
29. Khamees, T., Flori, R.E., Wei, M., 2017. Simulation Study of In-Depth Gel Treatment in Heterogeneous Reservoirs with Sensitivity Analyses. Presented at the SPE Western Regional Meeting, OnePetro. <https://doi.org/10.2118/185716-MS>
30. Khamees, T., Flori, R.E., Wei, M., n.d. Simulation Study of In-Depth Gel Treatment in Heterogeneous Reservoirs with Sensitivity Analyses 23.
31. Khan, M., Khoker, F., Husain, M., Ahmed, M., Anwar, S., 2018. Academ J Polym Sci Effects of Nanoparticles on Rheological Behavior of Polyacrylamide Related to Enhance Oil Recovery. *Journal of Polymer Science AJOP*.MS.ID.555573 (2018). <https://doi.org/10.19080/AJOP.2018.01.555573>
32. Koh, H., Lee, V.B., Pope, G.A., 2016. Experimental Investigation of the Effect of Polymers on Residual Oil Saturation. Presented at the SPE Improved Oil Recovery Conference, OnePetro. <https://doi.org/10.2118/179683-MS>
33. Kong, X., Ohadi, M.M., 2010. Applications of Micro and Nano Technologies in the Oil and Gas Industry-An Overview of the Recent Progress. Presented at the Abu Dhabi International Petroleum Exhibition and Conference, OnePetro. <https://doi.org/10.2118/138241-MS>
34. Kroon, M., Wegdam, G.H., Sprik, R., 1996. Dynamic light scattering studies on the sol-gel transition of a suspension of anisotropic colloidal particles. *Phys. Rev. E* 54, 6541–6550. <https://doi.org/10.1103/PhysRevE.54.6541>
35. Lake, L.W., 1989. Enhanced oil recovery. Prentice Hall, Englewood Cliffs, N.J.
36. Lee, J.H., Lee, K.S., 2013. Performance of Gel Treatments in Reservoirs with Multiscale Heterogeneity. *Journal of Chemistry* 2013, e416328. <https://doi.org/10.1155/2013/416328>
37. Lee, S., Kim, D.H., Huh, C., Pope, G.A., 2009. Development of a Comprehensive Rheological Property Database for EOR Polymers. Presented at the SPE Annual Technical Conference and Exhibition, OnePetro. <https://doi.org/10.2118/124798-MS>
38. Li, Z., 2015. Modelling and simulation of polymer flooding, including the effects of fracturing (Thesis). <https://doi.org/10.15781/T28M48>
39. Liauh, W.W., Liu, T.W., 1984. A Capillary Viscometer for the Study of EOR Polymers. Presented at the SPE Enhanced Oil Recovery Symposium, OnePetro. <https://doi.org/10.2118/12649-MS>
40. Lin, Y., Qin, H., Guo, J., Chen, J., 2021. Study on the Rheological Behavior of a Model Clay Sediment. *JMSE* 9, 81. <https://doi.org/10.3390/jmse9010081>
41. Lohne, A., 2020, IORCoreSim - combined EOR and SCAL simulator (Version 1.315) 201.
42. Lohne, A., Nødland, O., Stavland, A., Hiorth, A., 2017. A model for non-Newtonian flow in porous media at different flow regimes. *Comput Geosci* 21, 1289–1312. <https://doi.org/10.1007/s10596-017-9692-6>
43. Lohne, A., Stavland, A., Hiorth, A., Brattekas, B., 2019. Core Scale Modeling of Polymer Gel Dehydration by Spontaneous Imbibition. *SPE Journal*. <https://doi.org/10.2118/190189-PA>

44. Mack, J.C., Smith, J.E., 1994. In-Depth Colloidal Dispersion Gels Improve Oil Recovery Efficiency. Presented at the SPE/DOE Improved Oil Recovery Symposium, OnePetro. <https://doi.org/10.2118/27780-MS>
45. Maghzi, A., Mohebbi, A., Kharrat, R., Ghazanfari, M.H., 2011. Pore-Scale Monitoring of Wettability Alteration by Silica Nanoparticles During Polymer Flooding to Heavy Oil in a Five-Spot Glass Micromodel. *Transport in Porous Media* 87, 653–664. <https://doi.org/10.1007/s11242-010-9696-3>
46. Massarweh, O., Abushaikha, A.S., 2021. A review of recent developments in CO₂ mobility control in enhanced oil recovery. *Petroleum*. <https://doi.org/10.1016/j.petlm.2021.05.002>
47. McElfresh, P., Holcomb, D., Ector, D., 2012. Application of Nanofluid Technology to Improve Recovery in Oil and Gas Wells. Presented at the SPE International Oilfield Nanotechnology Conference and Exhibition, OnePetro. <https://doi.org/10.2118/154827-MS>
48. Mohammed, M., Babadagli, T., 2015. Wettability alteration: A comprehensive review of materials/methods and testing the selected ones on heavy-oil containing oil-wet systems. *Adv Colloid Interface Sci* 220, 54–77. <https://doi.org/10.1016/j.cis.2015.02.006>
49. Mongondry, P., Tassin, J.F., Nicolai, T., 2005. Revised state diagram of Laponite dispersions. *Journal of Colloid and Interface Science* 283, 397–405. <https://doi.org/10.1016/j.jcis.2004.09.043>
50. Mouchid, A., Lécolier, E., Van Damme, H., Levitz, P., 1998. On Viscoelastic, Birefringent, and Swelling Properties of Laponite Clay Suspensions: Revisited Phase Diagram. *Langmuir* 14, 4718–4723. <https://doi.org/10.1021/la980117p>
51. Negin, C., Ali, S., Xie, Q., 2017. Most common surfactants employed in chemically enhanced oil recovery. *Petroleum* 3, 197–211. <https://doi.org/10.1016/j.petlm.2016.11.007>
52. Nolan, D.P., 2011. 1 - Introduction, in Nolan, D.P. (Ed.), *Handbook of Fire and Explosion Protection Engineering Principles*. William Andrew Publishing, Oxford, pp. 1–11. <https://doi.org/10.1016/B978-1-4377-7857-1.00001-X>
53. NPD, 2021. Improve IOR/EOR Competence: en/force/improved-oil-and-gas-recovery/improve-eor-competence-test/ (accessed 6.1.21).
54. Peng, B., Zhang, L., Luo, J., Wang, P., Ding, B., Zeng, M., Cheng, Z., 2017. A review of nanomaterials for nanofluid enhanced oil recovery. *RSC Adv.* 7, 32246–32254. <https://doi.org/10.1039/C7RA05592G>
55. Pujala, R.K., 2014. *Dispersion Stability, Microstructure and Phase Transition of Anisotropic Nanodiscs*. Springer.
56. Pujari, S., Dougherty, L., Mobuchon, C., Carreau, P.J., Heuzey, M.-C., Burghardt, W.R., 2011. X-ray scattering measurements of particle orientation in a sheared polymer/clay dispersion. *Rheol Acta* 50, 3–16. <https://doi.org/10.1007/s00397-010-0492-3>
57. Rezazadeh, B., Sirousazar, M., Abbasi-Chianeh, V., Kheiri, F., 2020. Polymer-clay nanocomposite hydrogels for molecular irrigation application. *Journal of Applied Polymer Science* 137, 48631. <https://doi.org/10.1002/app.48631>

58. Rich, J.P., McKinley, G.H., Doyle, P.S., 2011. Size dependence of microprobe dynamics during gelation of a discotic colloidal clay.
59. Roussennac, B., Toschi, C., 2010. Brightwater® Trial in Salema Field (Campos Basin, Brazil). Presented at the SPE EUROPEC/EAGE Annual Conference and Exhibition, OnePetro. <https://doi.org/10.2118/131299-MS>
60. Ruzicka, B., Zaccarelli, E., Zulian, L., Angelini, R., Sztucki, M., Moussaïd, A., Narayanan, T., Sciortino, F., 2011. Observation of Empty Liquids and Equilibrium Gels in a Colloidal Clay. *Nature materials* 10, 56–60. <https://doi.org/10.1038/nmat2921>
61. Scott, T., Roberts, L.J., Sharp, S.R., Clifford, P.J., Sorbie, K.S., 1987. In-Situ Gel Calculations in Complex Reservoir Systems Using a New Chemical Flood Simulator. *SPE Reservoir Engineering* 2, 634–646. <https://doi.org/10.2118/14234-PA>
62. Seright, R., Brattekas, B., 2021. Water shutoff and conformance improvement: an introduction. *Pet. Sci.* 18, 450–478. <https://doi.org/10.1007/s12182-021-00546-1>
63. Seright, R.S., 1997. Use of Preformed Gels for Conformance Control in Fractured Systems. *SPE Production & Facilities* 12, 59–65. <https://doi.org/10.2118/35351-PA>
64. Seright, R.S., Fan, T., Wavrik, K., Balaban, R. de, 2010. New Insights into Polymer Rheology in Porous Media. Presented at the SPE Improved Oil Recovery Symposium, OnePetro. <https://doi.org/10.2118/129200-MS>
65. Shahin, A., Joshi, Y.M., 2012. Physicochemical Effects in Aging Aqueous Laponite Suspensions. *Langmuir* 28, 15674–15686. <https://doi.org/10.1021/la302544y>
66. Skrettingland, K., Dale, E., Stenerud, V., Lambertsen, A., Kulkarni, K., Fevang, O., Stavland, A., 2014. Snorre In-depth Water Diversion Using Sodium Silicate - Large Scale Interwell Field Pilot. Society of Petroleum Engineers - SPE EOR Conference at Oil and Gas West Asia 2014: Driving Integrated and Innovative EOR. <https://doi.org/10.2118/169727-MS>
67. Stosur, G.J., Hite, J.R., Carnahan, N.F., Miller, K., 2003. The Alphabet Soup of IOR, EOR and AOR: Effective Communication Requires a Definition of Terms. Presented at the SPE International Improved Oil Recovery Conference in the Asia Pacific, OnePetro. <https://doi.org/10.2118/84908-MS>
68. Suleimanov, B., Ismayilov, F., Veliyev, E., 2011. Nanofluid for enhanced oil recovery. *Journal of Petroleum Science and Engineering - J PET SCI ENGINEERING* 78, 431–437. <https://doi.org/10.1016/j.petrol.2011.06.014>
69. Sun et al. - 2020 - Combining Preformed Particle Gel and Curable Resin.
70. Taber, J.J., Martin, F.D., Seright, R.S., 1997. EOR Screening Criteria Revisited—Part 2: Applications and Impact of Oil Prices. *SPE Reservoir Engineering* 12, 199–206. <https://doi.org/10.2118/39234-PA>
71. Temizel, C., Putra, D., Peksaglam, Z., Susuz, O., Balaji, K., Suhag, A., Ranjith, R., Zhang, M., 2016. Production Optimization under Injection of Biopolymer, Synthetic Polymer and Gels in a Heterogeneous Reservoir. Presented at the SPE Eastern Regional Meeting, OnePetro. <https://doi.org/10.2118/184079-MS>
72. Adijats thesis 2019.
73. Thomas, S., 2008. Enhanced Oil Recovery - An Overview. *Oil & Gas Science and Technology - Rev. IFP* 63, 9–19. <https://doi.org/10.2516/ogst:2007060>

74. Tiwari, A., Hihara, L., Rawlins, J., 2014. *Intelligent Coatings for Corrosion Control*. Butterworth-Heinemann.
75. Tsau, J.S., Hill, A.D., Sepehrnoori, K., 1985. Modelling of Permeability Reducing Vertical Conformance Treatments. Presented at the SPE Oilfield and Geothermal Chemistry Symposium, OnePetro. <https://doi.org/10.2118/13569-MS>
76. van der Schaaf, U., Schütz, L., Karbstein, H., 2016. Interfacial and emulsifying properties of citrus pectin: Interaction of pH, ionic strength and degree of esterification. *Food Hydrocolloids* 62. <https://doi.org/10.1016/j.foodhyd.2016.08.016>
77. Vishnyakov, V., Suleimanov, B., Salmanov, A., Zeynalov, E., 2019. *Primer on Enhanced Oil Recovery*. Gulf Professional Publishing.
78. Wang, D., Xia, H., Liu, Z., Yang, Q., 2001. Study of the Mechanism of Polymer Solution With Visco-Elastic Behavior Increasing Microscopic Oil Displacement Efficiency and the Forming of Steady Oil Thread Flow Channels. Presented at the SPE Asia Pacific Oil and Gas Conference and Exhibition, OnePetro. <https://doi.org/10.2118/68723-MS>
79. Wehle, M.A., 2013 OMV Exploration & Production GmbH pages 151.
80. Youssif, M.I., El-Maghraby, R.M., Saleh, S.M., Elgibaly, A., 2018. Silica nanofluid flooding for enhanced oil recovery in sandstone rocks. *Egyptian Journal of Petroleum* 27, 105–110. <https://doi.org/10.1016/j.ejpe.2017.01.006>
81. Yuan, C., Pu, W., Varfolomeev, M.A., Wei, J., Zhao, S., Cao, L.-N., 2019. Deformable Micro-Gel for EOR in High-Temperature and Ultra-High-Salinity Reservoirs: How to Design the Particle Size of Micro-Gel to Achieve its Optimal Match with Pore Throat of Porous Media. Presented at the Abu Dhabi International Petroleum Exhibition & Conference, OnePetro. <https://doi.org/10.2118/197804-MS>
82. Yuan, S., Han, D., Wang, Q., Yang, H., 2000a. Numerical Simulation Study on Weak Gel Injection. Presented at the SPE Asia Pacific Oil and Gas Conference and Exhibition, OnePetro. <https://doi.org/10.2118/64291-MS>
83. Yuan, S., Han, D., Wang, Q., Yang, H., 2000b. Numerical Simulation Study on Weak Gel Injection. Presented at the SPE Asia Pacific Oil and Gas Conference and Exhibition, OnePetro. <https://doi.org/10.2118/64291-MS>
84. Yuan, S., Han, D., Wang, Q., Yang, H., 2000c. Numerical Simulator for the Combination Process of Profile Control and Polymer Flooding. Presented at the International Oil and Gas Conference and Exhibition in China, OnePetro. <https://doi.org/10.2118/64792-MS>
85. Zamani, N., Bondino, I., Kaufmann, R., Skauge, A., 2015. Effect of porous media properties on the onset of polymer extensional viscosity. *Journal of Petroleum Science and Engineering* 133, 483–495. <https://doi.org/10.1016/j.petrol.2015.06.025>
86. Zerkhalov, G., 2015. *Polymer Flooding for Enhanced Oil Recovery* <http://large.stanford.edu/courses/2015/ph240/zerkalov1>
87. Zhou, Y., Wu, X., Zhong, X., Reagen, S., Zhang, S., Sun, W., Pu, H., Xiaojun Zhao, J., 2020. Polymer nanoparticles based nano-fluid for enhanced oil recovery at harsh formation conditions. *Fuel* 267, 117251. <https://doi.org/10.1016/j.fuel.2020.117251>
88. Zhu, J., Zhao, H., Cao, G., Banjar, H., Zhu, H., Peng, J., Zhang, H.-Q., 2021. A New Mechanistic Model for Emulsion Rheology and Boosting Pressure Prediction in

Electrical Submersible Pumps (ESPs) under Oil-Water Two-Phase Flow. SPE Journal
26, 667–684. <https://doi.org/10.2118/196155-PA>